INTERNATIONAL JOURNAL OF CLIMATOLOGY
Int. J. Climatol. (2017)
Published online in Wiley Online Library
(wileyonlinelibrary.com) DOI: 10.1002/joc.5176

Recent changes in monthly surface air temperature over Peru, 1964–2014

Sergio M. Vicente-Serrano,[a*] Juan I. López-Moreno,[a] Kris Correa,[b] Grinia Avalos,[b] Juan Bazo,[c] Cesar Azorin-Molina,[d] Fernando Domínguez-Castro,[a] Ahmed El Kenawy,[e] Luis Gimeno[f] and Raquel Nieto[f]

[a] *Instituto Pirenaico de Ecología, Consejo Superior de Investigaciones Científicas (IPE-CSIC), Zaragoza, Spain*
[b] *Dirección de Climatología, Servicio nacional de Meteorología e Hidrología (SENAMHI), Lima, Peru*
[c] *Red Cross/Red Crescent Climate Centre, The Hague, Netherlands*
[d] *Regional Climate Group, Department of Earth Sciences, University of Gothenburg, Sweden*
[e] *Department of Geography, Mansoura University, Egypt*
[f] *Environmental Physics Laboratory (EPhysLab), Facultade de Ciencias, Universidade de Vigo, Ourense, Spain*

ABSTRACT: This study assessed changes in the maximum and minimum surface air temperatures across Peru during the period 1964–2014. For this purpose, we employed the most complete records of air temperature series that were also subjected to a rigorous quality control and homogenization protocol. Based on the homogenized series, we created a monthly gridded data set of maximum and minimum air temperatures at a 5 × 5 km grid spacing. The results suggest a general warming trend in surface air temperature across Peru, albeit with clear spatial and seasonal variation. Our results also reveal some differences in the detectable trends between maximum and minimum air temperatures. Maximum air temperature trends mainly increased during the austral summer (DJF), but cold season minimum air temperature trends showed an opposite pattern, with the strongest warming being recorded in the austral winter (JJA). In addition, maximum air temperature trends exhibited a clear elevation-warming dependency, with the strongest warming recorded at highly elevated sites. On the contrary, this dependency is weakened for minimum air temperature trends, as lower magnitudes of change and even a cooling trend were observed at high elevations during most months of the year. For mean air temperature trends, there are no clear spatial and temporal seasonal differences across Peru.

KEY WORDS air temperature; trends; elevation; warming; Andes; Pacific coastland; Altiplano

Received 19 October 2016; Revised 16 May 2017; Accepted 17 May 2017

1. Introduction

Global warming is a key feature of the recent changing climate, which is mainly linked to a range of climate change processes, such as changes in the atmospheric circulation (e.g. Yin, 2005; Vecchi *et al.*, 2006; Vecchi and Soden, 2007), relative humidity (e.g. Simmons *et al.*, 2010; Willett *et al.*, 2014), evapotranspiration (e.g. Goyal, 2004; Abtew and Melesse, 2013), the atmospheric evaporative demand (e.g. Wang *et al.*, 2012; Vicente-Serrano *et al.*, 2014; Azorin-Molina *et al.*, 2015) and droughts (e.g. Burke, 2011; Dai, 2011) besides other numerous hydrological, agricultural and environmental impacts (Vörösmarty *et al.*, 2000; Walther *et al.*, 2002; Parmesan and Yohe, 2003). On average, the global air temperature has increased by 0.8 °C in the past six decades (Hartmann *et al.*, 2013). Nevertheless, this pattern is not homogeneous globally, where some regions show a higher warming trend (Hartmann *et al.*, 2013). This feature is also evident at the regional and local scales in many areas worldwide (e.g. Gonzalez-Hidalgo *et al.*, 2016; Kunkel *et al.*, 2015; Dai *et al.*, 2016). These spatial differences are mainly attributed to microclimatic features, topographic gradients, distance to seas and oceans and the influence of different atmospheric circulation patterns. A number of studies have also suggested remarkable differences in the warming rate over many mountainous chains, confirming that these complex terrain regions are among the most vulnerable regions to climate change and variability worldwide (Beniston *et al.*, 1997; Giorgi *et al.*, 1997; Pepin and Lundquist, 2008; El Kenawy *et al.*, 2013; Wang *et al.*, 2014).

Nowadays, a range of studies have analysed recent trends in air temperature in many regions, ranging from regional (e.g. Brunetti *et al.*, 2006; Martínez *et al.*, 2010), continental or hemispherical (e.g. Jones *et al.*, 2012) to the whole earth (e.g. Hartmann *et al.*, 2013). In many cases, these studies employ low density of meteorological stations. These limitations make it necessary to use the most complete possible climate observations in any region in order to provide a detailed spatial picture of temperature

* Correspondence to: S. M. Vicente-Serrano, Instituto Pirenaico de Ecología, Consejo Superior de Investigaciones Científicas (IPE-CSIC), Campus de Aula Dei, P.O. Box 13034, E-50059 Zaragoza, Spain. E-mail: svicen@ipe.csic.es

changes. In South America, a number of studies have assessed recent changes in air temperature using the available complete, quality controlled and homogenized data (e.g. Villalba *et al.*, 2003; Falvey and Garreaud, 2009; Barros *et al.*, 2015; Bennett *et al.*, 2016). In the Andes, some studies have comprehensively analysed recent trends in air temperature using high-quality data (e.g. Vuille *et al.*, 2000, 2015). One example is Seiler *et al.* (2013) who analysed air temperature trends from 29 stations in Bolivia for the period 1960–2009, suggesting an increase in air temperature on the order of 0.1 °C decade^{-1}. Spatially, the notable increase in air temperature was observed in the Andes, particularly during the dry season. More recently, Morán-Tejeda *et al.* (2016) assessed the evolution of air temperature over Ecuador, indicating an intense warming trend in the entire country, except for maximum air temperature along the coastal region.

In some areas of the Andean region, the knowledge related to the tendency of air temperature is still lacking, motivating investigations that determine the magnitude of the recent warming in air temperature at a more detailed spatial scale (McPhaden *et al.*, 2010). Peru is the biggest Andean country in South America (1.28×10^6 km^2) and represents one of the most vulnerable to climate change worldwide (Carey, 2005). It shows noticeable geographic and climatic contrasts between the Pacific coastland, the Andes and the Amazonian area. In particular, the Pacific region is very dry, as a consequence of dominant cold Pacific sea surface temperature. On the other hand, the Andes exhibits important climatic and ecological variations, mainly related to the strong contrasts in elevation and terrain aspects (García, 1994) as well as the influence of different circulation mechanisms (Garreaud, 2009; Garreaud *et al.*, 2009). Given the strong dependence of agricultural activities and human livelihood on climate variability and change in the region, a comprehensive assessment of the recent air temperature trends in Peru is required for a range of disciplines spanning agriculture, water resource planning and management, and flood assessments in the region.

Although some studies have analysed recent air temperature trends in Peru, they have been specific to some parts of the country, mostly the mountainous massifs (Mark and Seltzer, 2005; Racoviteanu *et al.*, 2008; Salzmann *et al.*, 2013; López-Moreno *et al.*, 2014; Schauwecker *et al.*, 2014; Veettil *et al.*, 2016) and the Peruvian–Bolivian Altiplano (Vuille *et al.*, 2000; Valdivia *et al.*, 2013; López-Moreno *et al.*, 2016). Over the Andean region, studies suggest a differential warming, as a function of elevation (Vuille and Bradley, 2000; Falvey and Garreaud, 2009; Vuille *et al.*, 2015). Nevertheless, there is no agreement either on the rates of warming for different elevations or on their spatial variations (Racoviteanu *et al.*, 2008; Vuille *et al.*, 2015; Bennett *et al.*, 2016).

In this study, we analyse the recent monthly and annual air temperature trends over Peru during the period 1964–2014, based on a new compiled gridded high-resolution data set that utilized observations from all available meteorological stations. The objectives of the study are (1) to quantify the trend in maximum, minimum and mean air temperatures and (2) to assess the response of air temperature changes to the altitudinal gradient in Peru.

2. Data and methods

2.1. Data set description

We used the complete records of air temperature available in the National Meteorological and Hydrological Service of Peru (Servicio Nacional de Meteorología e Hidrología, SENAMHI). Air temperature is measured by maximum/minimum thermometers located inside Stevenson screens following recommendations by the World Meteorological Organisation. This data set included more than 300 stations that cover vast areas of the country (Figure 1), with the exception of the Amazon rainforest in the north and the east, where the density of population is very low and the meteorological stations are thus scarce. In contrast, the coastland area and the majority of the Andes have a good coverage of stations measuring air temperature. An important aspect of the temperature network in Peru is that the coverage of the available data series varies considerably over time across the country. Before the 1960s, there were very few data available in Peru (Figure 2). However, 1964 was markedly a transition year, where a number of new meteorological stations were set up throughout the territory. By the second half of the 1960s, more than 100 stations have been available in Peru, and this number was maintained during the 1970s, but decreased in the 1980s, as a consequence of the social and political instability in the country. While the number of stations increased sharply during the 1990s and the beginning of the 2000s, it remained constant ($N = 250$) from then on.

Overall, the evolution of the number of stations and their spatial coverage combined together to determine the selection of the study period from 1964 to 2014. In this regard, we restricted our analysis to stations with no more than 20% of missing data over the study period. The main geographic characteristics of the selected stations ($N = 99$) are listed in Table 1 and their spatial distribution is illustrated in Figure 1.

2.2. Quality control and homogenization

The monthly maximum and minimum air temperature series in the selected meteorological stations were subjected to a robust quality control and homogenization. The quality control procedure was based on the comparison of the percentile rank of each data record with the average percentile rank of the data recorded at adjacent stations (Vicente-Serrano *et al.*, 2010), considering a threshold of 0.8 deciles. The temporal homogeneity of the series was analysed using a relative homogeneity method (Venema *et al.*, 2012). For this purpose, we used a recently developed relative homogeneity method (HOMER – HOMogenization software in R), which compares each candidate series with a number of available

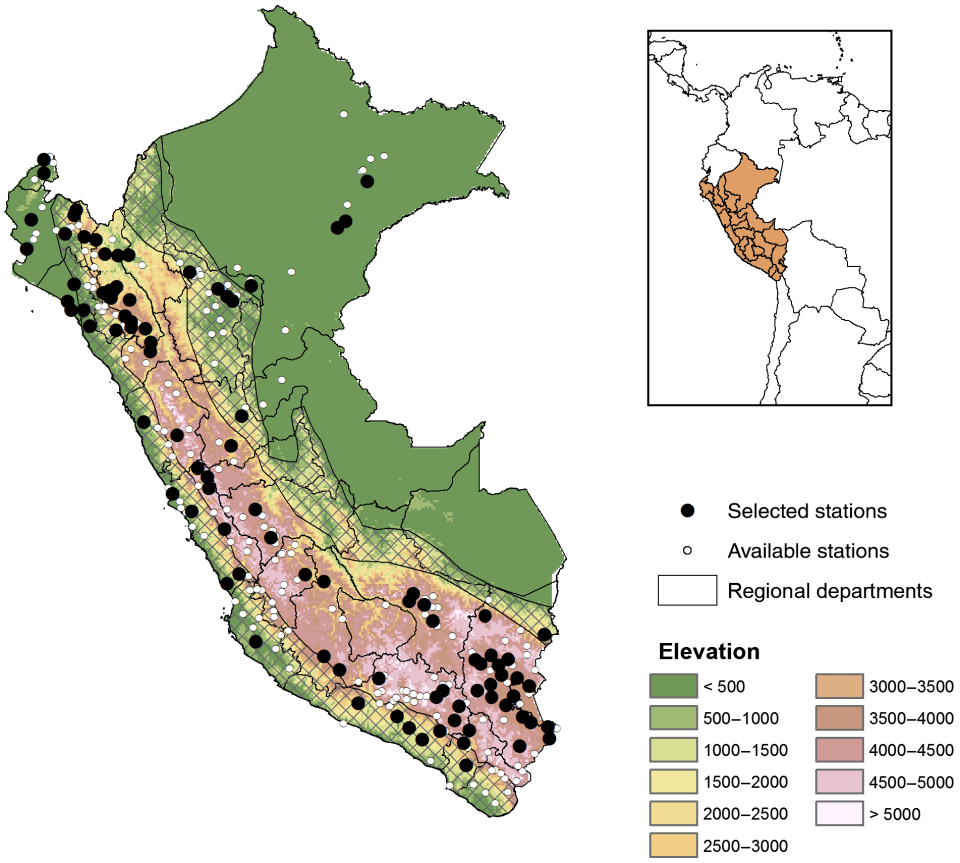

Figure 1. Spatial distribution of all and the selected meteorological stations with air temperature data available for the period 1964–2014. Masked areas represent the west and east slopes of the Peruvian Andes, which were analysed independently. [Colour figure can be viewed at wileyonlinelibrary .com].

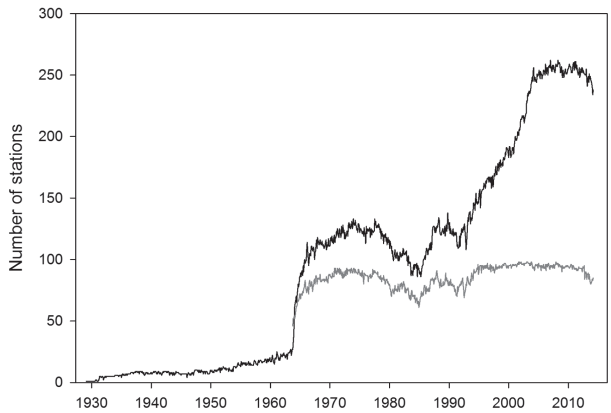

Figure 2. Black line: temporal evolution of air temperature data availability in Peru. Grey line: availability of data from the set of selected stations for 1964–2014.

series (Mestre *et al.*, 2013). HOMER is a semi-automatic methodology that combines a fully automatic joint segmentation with a partly subjective pairwise comparison and includes some of the techniques recommended after an intercomparison study of homogenization procedures (Venema *et al.*, 2012). Testing inhomogeneities for each maximum and minimum air temperature series was made using the closest 10 stations to each candidate station. The segmentation analysis was based on annual and seasonal data. This method provides an estimation of break points in the time series relative to neighbouring stations and indicates high probabilities of the presence of inhomogeneities. Thus, if a break point was identified between a station and a number of neighbouring stations for the same season/year, it was considered probable that there was an inhomogeneity in the series.

Figure 3 shows the temporal evolution of the number of inhomogeneities introduced in the entire data set during the period 1964–2014. The maximal number of inhomogeneities was found for maximum air temperature in 1964 (9) and for minimum air temperature in 1983 (8). A lower number of inhomogeneities is recorded from 2000 in comparison to earlier times. In general, the number of inhomogeneities found is higher for maximum than for minimum air temperature series. Overall, the stations free from inhomogeneities or affected by only one break are dominant. Very few meteorological stations have been affected by three or more inhomogeneities during the study period. In the following procedure, HOMER corrected the inhomogeneities and completed missing values based on Equation (8) reported by Mestre *et al.* (2013). Figure S1 (Supporting information) shows the percentage of data in each station that was replaced by the homogeneity procedure and the percentage of missing data

Table 1. The main characteristics of the selected meteorological stations used in this work.

Id.	Station	Latitude (°)	Longitude (°)	Elevation (m.a.s.l.)	Id.	Station	Latitude (°)	Longitude (°)	Elevation (m.a.s.l.)
1	Ricaplaya	−3.813	−80.458	49	51	Canete	−13.075	−76.331	101
2	Puertopizarro	−3.508	−80.457	1	52	Huayao	−12.034	−75.339	3376
3	Tamshiyacu	−4.003	−73.161	106	53	Pacaran	−12.862	−76.055	712
4	Mallares	−4.864	−80.746	39	54	Acobamba	−12.864	−74.559	3056
5	Chusis	−5.525	−80.847	6	55	Laquinua	−13.034	−74.135	3490
6	Moroccan	−5.184	−79.984	119	56	Urubamba	−13.304	−72.125	3137
7	Ayabaca	−4.644	−79.729	2552	57	Antaancachuro	−13.468	−72.216	3320
8	Sausaldeculucan	−4.763	−79.779	1916	58	Acomayo	−13.917	−71.684	3634
9	Huancabamba	−5.250	−79.550	3094	59	Ollachea	−13.804	−70.498	3092
10	Tabaconas	−5.322	−79.288	2256	60	Riogrande	−14.542	−75.220	305
11	Chontali	−5.644	−79.085	1715	61	Sancamilo	−14.068	−75.729	430
12	Jaen	−5.678	−78.779	726	62	Puno	−15.823	−70.018	3947
13	Baguachica	−5.661	−78.542	535	63	Puquio	−14.712	−74.136	2550
14	Requena	−5.043	−73.836	142	64	Coracora	−15.017	−73.784	3300
15	Genaroherrera	−4.900	−73.650	125	65	Caraveli	−15.771	−73.362	1781
16	Lambayeque	−6.704	−79.921	12	66	Cotahuasi	−15.211	−72.894	2934
17	Augustoweberbauer	−7.167	−78.485	2680	67	Sibayo	−15.486	−71.453	4057
18	Elporvenir	−6.593	−76.322	204	68	Chivay	−15.638	−71.597	3642
19	Cayalti	−6.898	−79.559	61	69	Pampahuta	−15.491	−70.678	4429
20	Talla	−7.271	−79.423	101	70	Chuquibambilla	−14.796	−70.728	3912
21	Reque	−6.898	−79.847	13	71	Imata	−15.837	−71.088	4450
22	Jayanca	−6.322	−79.779	83	72	Ayaviri	−14.881	−70.593	4119
23	Llama	−6.515	−79.123	2411	73	Progreso	−14.695	−70.356	3908
24	Huambos	−6.458	−78.966	2296	74	Lampa	−15.356	−70.373	3859
25	Santacruz	−6.627	−78.949	2034	75	Cabanillas	−15.639	−70.346	3886
26	Cutervo	−6.379	−78.816	2699	76	Azangaro	−14.915	−70.191	3866
27	Cochabamba	−6.461	−78.889	2073	77	Arapa	−15.136	−70.119	3961
28	Contumaza	−7.356	−78.830	2811	78	Munani	−14.779	−69.966	3915
29	Granjaporcon	−7.034	−78.627	3151	79	Huancane	−15.203	−69.763	3818
30	Bambamarca	−6.678	−78.525	2663	80	Huarayamoho	−15.390	−69.491	3894
31	Sanjuan	−7.288	−78.491	2106	81	Capachica	−15.616	−69.844	3819
32	Sanmarcos	−7.322	−78.169	2684	82	Tambopata	−14.220	−69.152	1860
33	Cajabamba	−7.627	−78.051	2669	83	Lajoya	−16.593	−71.919	1281
34	Huamachuco	−7.830	−78.051	3456	84	Pampademajes	−16.328	−72.211	1432
35	Rioja	−6.047	−77.167	819	85	Moquegua	−17.169	−70.932	1470
36	Lamas	−6.424	−76.525	480	86	Puntaatico	−16.229	−73.694	375
37	Sauce	−6.694	−76.203	727	87	Aplao	−16.069	−72.491	1625
38	Navarro	−6.356	−75.779	165	88	Lapampilla	−16.403	−71.517	2435
39	Huanuco	−9.966	−76.237	1923	89	Ilo	−17.627	−71.288	357
40	Buenavista	−9.434	−78.200	335	90	Elfrayle	−16.155	−71.189	4153
41	Recuay	−9.729	−77.454	3589	91	Omate	−16.678	−70.983	2377
42	Tingomaria	−9.288	−76.000	656	92	Ubinas	−16.383	−70.857	3432
43	Alcantarilla	−11.050	−77.550	143	93	Yacango	−17.094	−70.866	2130
44	Huayan	−11.450	−77.117	396	94	Samagrande	−17.784	−70.488	532
45	Cajatambo	−10.467	−76.984	4566	95	Mazocruz	−16.746	−69.712	3995
46	Oyon	−10.667	−76.767	3696	96	Ilave	−16.085	−69.644	3842
47	Picoy	−10.917	−76.734	3853	97	Juli	−16.203	−69.457	3880
48	Matucana	−11.839	−76.378	2512	98	Tahuaco-Yunguyo	−16.305	−69.068	3834
49	Tarma	−11.397	−75.690	3654	99	Desaguadero	−16.569	−69.040	3843
50	Granjakcayra	−13.557	−71.875	3251					

that were complete for both maximum and minimum air temperature. A majority of stations showed no changes and only a small percentage of them exhibited a high percentage of data replaced to correct inhomogeneities.

2.3. Gridded air temperature data set

Using the complete quality controlled and homogenized air temperature data set for 99 meteorological stations in Peru, we created a gridded monthly data set of maximum and minimum air temperature at a spatial resolution of 5×5 km. For this purpose, we used a regression-based approach following Ninyerola *et al.* (2000). This approach makes use of a range of geographic and topographic variables that likely control the spatial distribution of air temperature. Numerous studies have employed a large number of predictors that are likely to explain the spatial variability

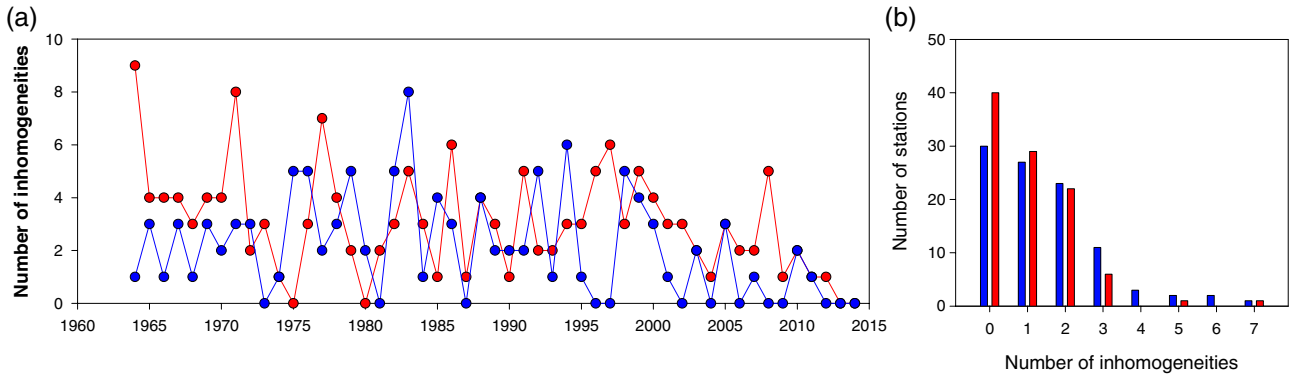

Figure 3. (a) Temporal evolution of the number of inhomogeneities recorded each year. (b) Number of inhomogeneities found in each station. Blue line represents minimum air temperature and red line represents maximum air temperature. [Colour figure can be viewed at wileyonlinelibrary.com].

of the climatic patterns (e.g. Basist *et al.*, 1994; Daly *et al.*, 1994, 2002; Agnew and Palutikof, 2000; Vicente Serrano *et al.*, 2003; El Kenawy *et al.*, 2010). In this study, we used the elevation at the spatial resolution of 5×5 km obtained from the Global Multi-resolution Terrain Elevation Data 2010 (https://lta.cr.usgs.gov/GMTED2010). We also used the geographic latitude and longitude and the distance to the oceans, as a measure of continentality influences. The raw data of these variables were also interpolated to a 5×5 km grid spacing. We did not apply any filtering of the elevation data to avoid any suspicious results (e.g. maximum air temperature becomes lower than the minimum air temperature). In the same context, while earlier works accounted for the possible effect of topographic barriers on climatic variables through using the maximum height within a wedge of a particular aspect and radius (e.g. Agnew and Palutikof, 2000; El Kenawy *et al.*, 2010), we found this approach inappropriate in our case, given the strong topographic complexity in Peru. This terrain complexity may introduce strong artificial boundaries, with no climatological meaning, between adjacent areas.

In this work, we created dependence models between the climate data (i.e. the mean maximum and minimum air temperatures) and the independent geographic and topographic variables for each month independently over the period 1964 and 2014. The value of a climate variable in any unsampled point is obtained, as:

$$z(x) = b0 + b1P1 + b2P2 + \ldots + bnPn \quad (1)$$

where z is the predicted value of the climate variable at point x, $b0, \ldots, bn$ are the regression coefficients and $P1, \ldots, Pn$ are the values of the different independent variables at point x.

Prior to applying the linear interpolation models, the normality of each independent variable was tested using the Kolmogorov–Smirnoff test, and natural logarithms were applied, when necessary, in order to fit a normal distribution more closely. For each independent month, we created a model using the independent variables. Nonetheless, to avoid the possible impact of collinearity, which is caused by intercorrelated independent variables, on the model skill, we applied a forward stepwise procedure with 'probability to enter' set to 0.05. This procedure allowed for defining the significant variables only, as recommended by Hair *et al.* (1998).

Figure 4 depicts the coefficients of determination (R^2) obtained for each month between 1964 and 2014 for maximum and minimum air temperature data and the normalized coefficients of the independent variables for each monthly model. In general, the coefficients of determination of the models are higher for minimum temperature than for maximum air temperature. In addition, results reveal certain seasonality, as the coefficients of determination were higher during the austral summer (DJF) than in austral winter (JJA) months. Models obtained for minimum air temperature showed a high predictive capacity of the spatial distribution of air temperature, with coefficients usually higher than 0.85. For maximum air temperature, the coefficients were close to 0.9 during summer, whereas the percentage of the variance in the spatial distribution of maximum air temperature during wintertime approached to 70%. Overall, the use of a maximum of four geographic/topographic predictors in the regression models was skilful in explaining almost 70% of the explained variance of maximum air temperature distribution in the study domain.

The normalized coefficients revealed important differences among the variables. Elevation showed the main explanatory capacity of the spatial distribution of both maximum and minimum temperatures. There is no clear seasonality in the contribution of elevation to explaining the air temperature distribution, with no clear differences between maximum and minimum air temperatures. The only exception was found during January, as the role of the elevation noticeably decreased for maximum air temperature. In contrast, other variables showed weaker impact on the obtained models.

The regression-based approach is an 'inexact' technique because the predicted value of the climatic variable z(x) does not coincide with the real data collected at weather stations. The errors introduced in the gridded layers can originate from some local climatic effects or the influence of other possible variables (predictors) that were not taken into account in the regression models. In general, these differences (errors) can be estimated at each point and particular procedures can then be performed to correct these

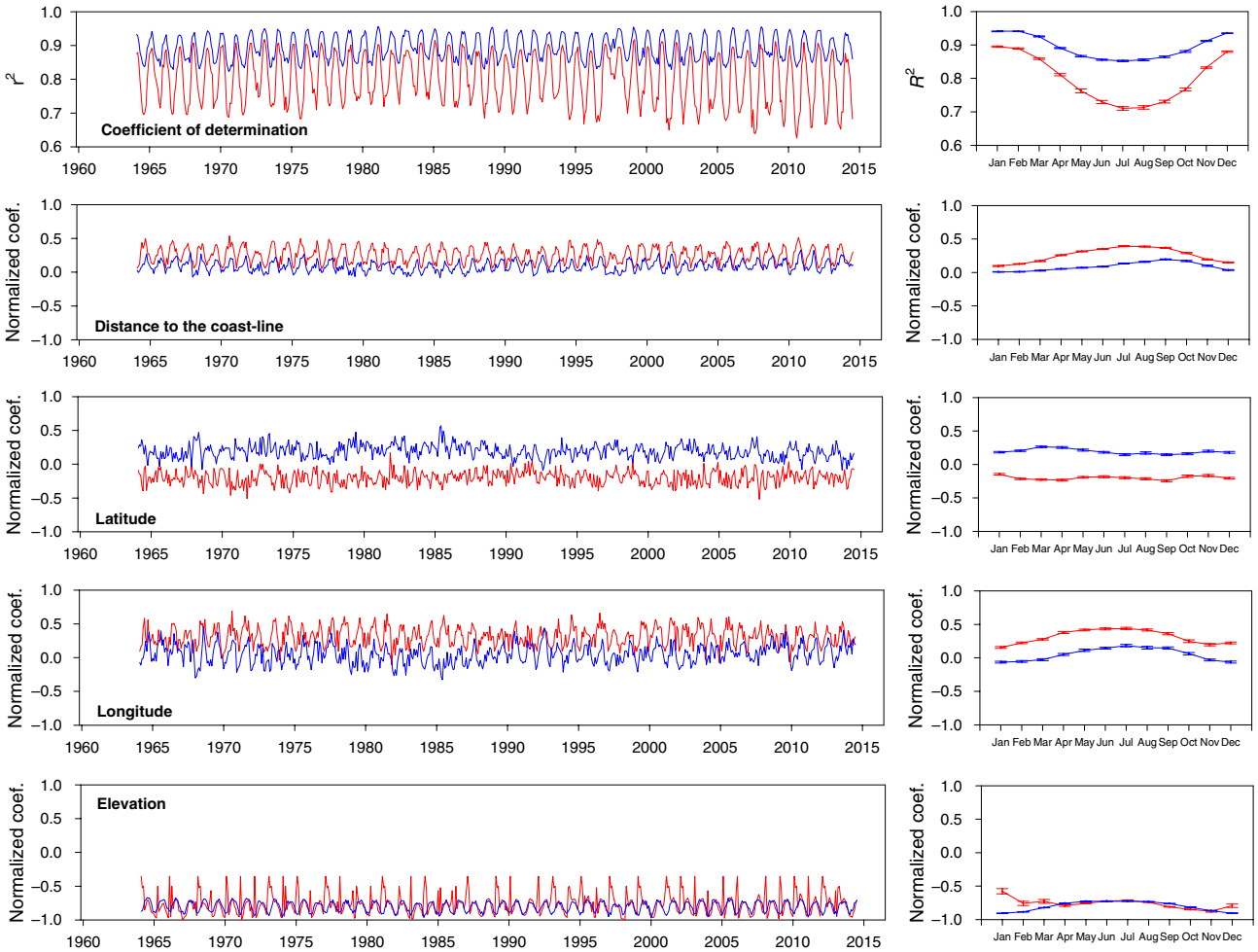

Figure 4. Temporal evolution and the monthly averages of the coefficient of determination (R^2) of the regression models used to obtain the gridded data and the normalized coefficients of the distance to the coastline, longitude, latitude and elevation. Red line represents maximum air temperature and blue line represents minimum air temperature. [Colour figure can be viewed at wileyonlinelibrary.com].

errors. The residual (i.e. the difference between the air temperature measured at a weather station and that predicted by the model) is obtained and interpolated over the entire territory using local interpolation techniques. In particular, we applied the inverse distance weighting algorithm to interpolate the residuals at the spatial resolution of 5×5 km. The final layers were obtained using the sum of the interpolated layers of residuals and the corresponding regression models. Our procedure has commonly been used in different earlier studies (e.g. Agnew and Palutikof, 2000; Ninyerola *et al.*, 2000; Brown and Comrie, 2002; Vicente-Serrano *et al.*, 2007).

The gridded layers were validated by means of a cross-validation method. In the absence of a sufficient number of observatories ($N = 99$) for the whole country, the 'jack-knifing' method was adopted. This method is based on withholding, in turn, one station out of the network, estimating regression coefficients from the remaining observatories, interpolating the residuals, calculating the sum of both and obtained the predicted maximum and minimum air temperature value in each withheld observatory for each month (Phillips *et al.*, 1992). This method has frequently been used in climatology (e.g. Daly *et al.*, 1994; Holdaway, 1996; El Kenawy *et al.*, 2010), particularly when dealing with a low number of cases for validation purposes.

In order to assess the skill of each regression model, we employed a set of validation measures that assess the differences and the spatial agreement between the values of air temperature recorded at the meteorological stations and those predicted at these sites using the 'jack-knifing' approach. Here, we used the mean bias error (MBE), which gives indications on whether the observed data are overestimated or underestimated using the interpolation algorithm. Also, we applied the mean absolute error (MAE), which is a measure of the average error of the interpolation. Another estimator is the Willmott's D (Willmott, 1982), which is a relative and bounded [−1 to 1] measure to assess the accuracy of predictions. Also, we used the Kling–Gupta efficiency (KGE) statistic, which is a model evaluation criterion that can be decomposed in the contribution of mean, variance and correlation to model performance. The use of a combination of accuracy estimators is advantageous, as it assesses the ability of the models to predict different aspects of the observed data (e.g. mean, standard deviation, variance, correlation and asymmetry).

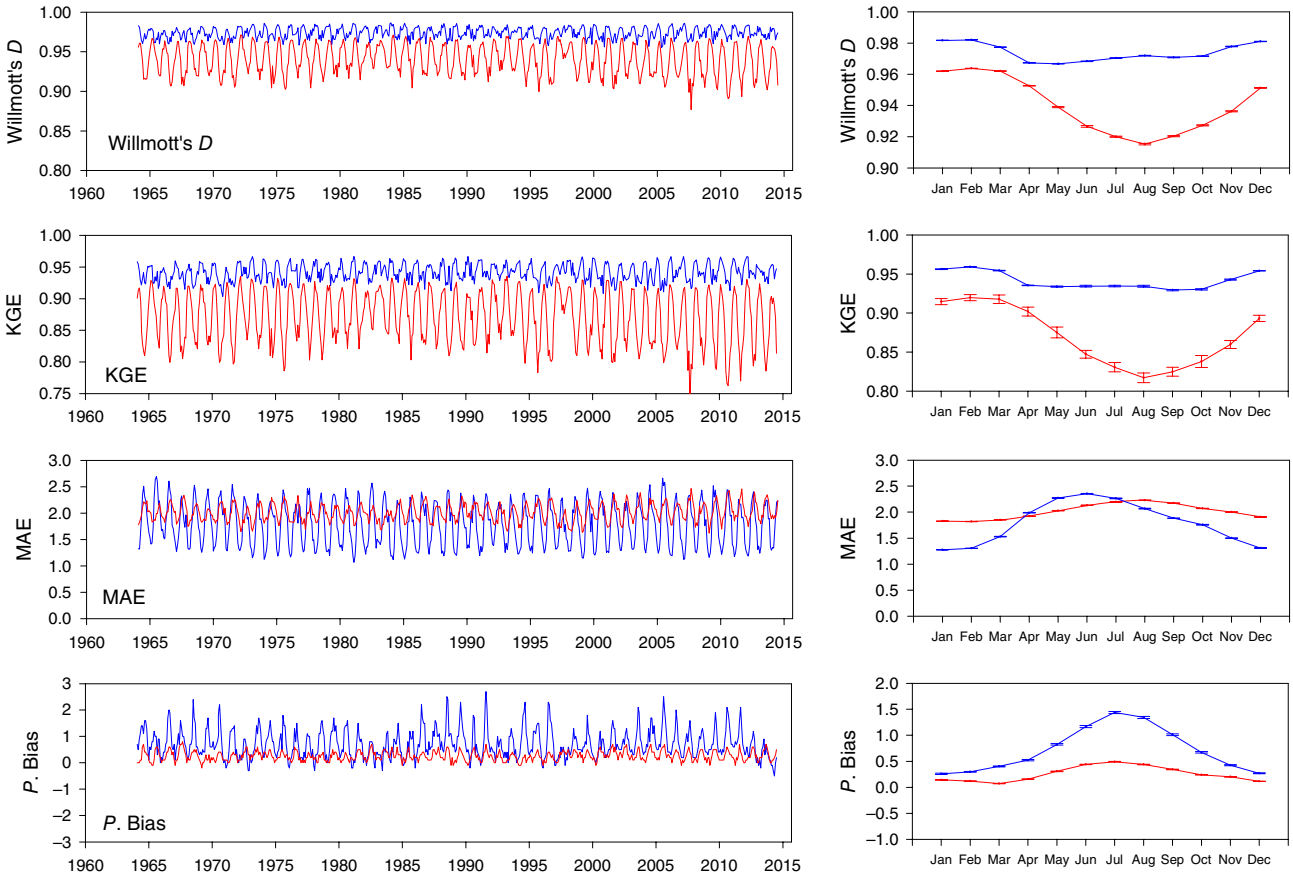

Figure 5. Temporal evolution and monthly averages of the error/accuracy statistics. Red line represents maximum air temperature and blue line represents minimum air temperature. [Colour figure can be viewed at wileyonlinelibrary.com].

Figure 5 summarizes the results of all validation statistics calculated for the different maximum and minimum air temperature grids. In general, all the obtained grids for air maximum and minimum temperatures had a high quality, given that the Willmott's *D* statistic showed values generally above 0.9 for the majority of the grids. This suggests a very good agreement between the observed and the predicted data. Similar to the results of R^2 (Figure 4), the results of the Willmott's *D* and KGE statistics showed a better quality for the minimum than for the maximum air temperature. At the seasonal scale, results suggest better quality for the austral summer than for austral winter months, particularly for maximum air temperature. As illustrated in Figure 5, the interannual variability of Willmott's *D* values is markedly low, especially for minimum air temperature: a finding that is also confirmed by KGE. The MAE values were generally close to 2 °C for maximum air temperature during all months of the year, with low interannual variations. MAE for minimum air temperatures showed a strong seasonality, with the highest errors recorded between April and August and the lowest in austral summer months, with average MAEs close to 1 °C. The bias of maximum air temperature grids is small. Bias results (*P* bias) indicate that the models tend to overestimate minimum air temperature, especially during the austral winter months. Overall, there are no noticeable interannual differences in this pattern. Notably, the bias results suggest better results for maximum air temperature than for minimum air temperature.

One of the main objectives of this study is to determine if there are any differences in air temperature trends that may be determined by the altitudinal gradient, with the purpose of determining the possible differential warming at different heights. For this reason, it was essential to evaluate the extent to which errors were introduced to the obtained gridded layers as a function of elevation over Peru. We analysed the relationship between the elevation and the difference of the predicted and the observed values for each meteorological observatory. We named this difference as residual and note that this residual is different and independent of that obtained in the interpolation procedure. Regardless of the month of the year, there is no clear distribution of the residuals controlled by elevation, either for the gridded maximum or minimum air temperature (Figures S2 and S3). This finding suggests that the residuals had no linear association with elevation over Peru. Instead, the errors resulted from the interpolation procedure were randomly distributed over space, regardless of the elevation. Moreover, there is not a systematic spatial bias in the errors obtained from maximum and minimum air temperatures (Figures S4 and S5) although the stations located in the Northwest and Southeast mountain areas tend to show higher average errors for maximum air temperatures and some stations close to the Pacific coastland

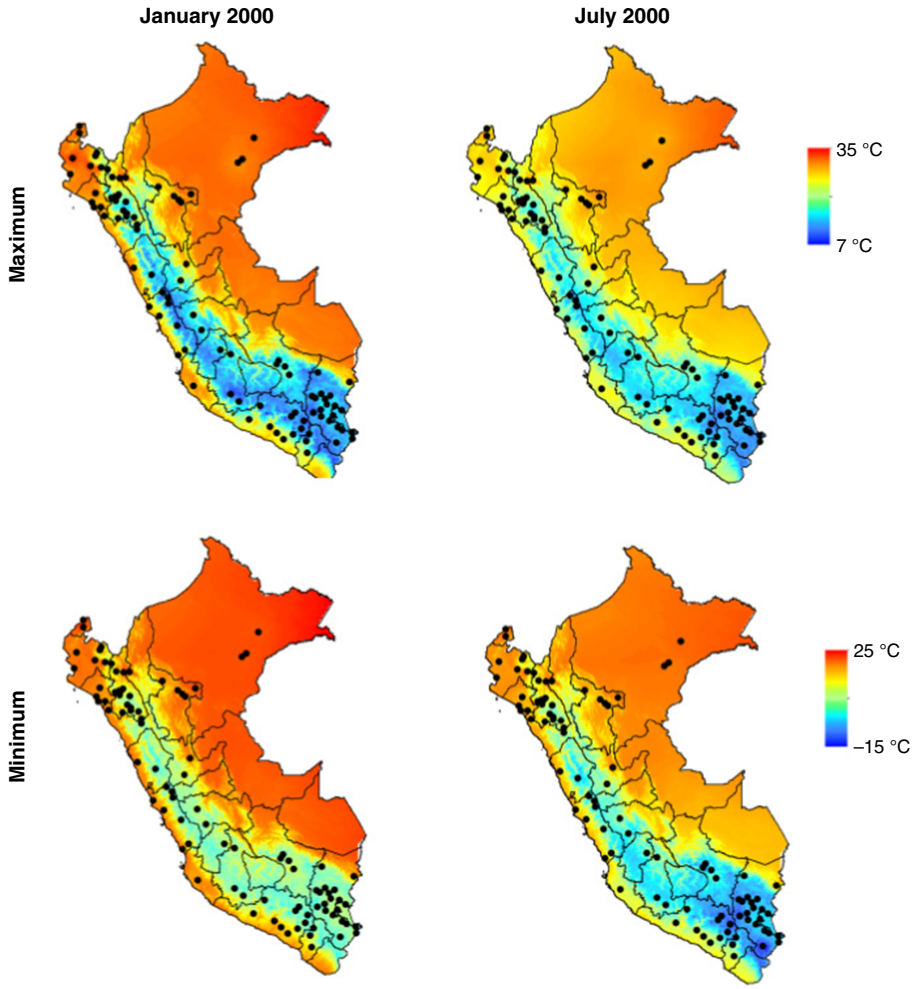

Figure 6. Examples of the 5 km gridded maximum and minimum air temperatures calculated for January and July 2000. [Colour figure can be viewed at wileyonlinelibrary.com].

also show higher errors in the minimum air temperature maps. In any case, these stations are usually located near other stations that show low MAE's, suggesting a spatial random distribution of errors. The complex terrain of Peru could be explaining these differences as determines several local climate characteristics.

Given the availability of air temperature records and the extremely complex topography of Peru, the gridded maximum and minimum air temperature can be considered of very good quality. The estimated errors are generally small and randomly distributed over space. Accordingly, our gridded data set can be useful for assessing the spatio-temporal variability of air temperature at a high spatial resolution. Nevertheless, there are regions, like most of the eastern Amazonian area, in which the availability of meteorological stations is small and in which the temperature predictions are uncertain. For this reason, in the maps of temperature trends these areas have been marked, considering a minimum threshold of 150 km to the closest meteorological station. Figure 6 gives an example of the spatial gridded layers of maximum and minimum air temperatures for the summer (January) and winter (July) of 2000. The gridded maps show the strong spatial gradients of air temperature, with a clear influence of topography on the distribution of both maximum and minimum air temperatures.

2.4. Trend analysis

We obtained the monthly and annual series of maximum, minimum and mean air temperatures for the whole Peru. Using the country regional series, the significance of the trends was analysed using the nonparametric Mann–Kendall tau coefficient. This statistic is more robust than parametric coefficients and does not assume any normality of the data series (Lanzante, 1996). Statistically significant differences were defined as those with p values <0.05. To avoid problems related to the temporal autocorrelation in the data, we used a modified Mann–Kendall trend test, returning the corrected p values after accounting for the temporal pseudoreplication (Hamed and Rao, 1998). To determine the trend, a linear regression between time (independent variable) and the temperature series (dependent variable) was used. The slope of each model indicates the trend, which was summarized in °C decade^{-1}.

We have also applied a jack-knife approach to the trend results, comparing the observed air temperature trend

in each station and the predicted trend considering the 'jack-knifing' predictions. We calculated both the magnitude and significance of the trend. A statistical test for the equality of regression slope coefficients was used (Paternoster *et al.*, 1998) to compare between the observed and predicted magnitude of air temperature trends assessed at a confidence interval of 95% ($p < 0.05$) (Table S1). The comparison shows that only eight, five and four stations for maximum, minimum and mean air temperature, respectively, showed a predicted annual air temperature trend significantly different considering observations and 'jack-knifing' predictions. The number of stations showing significant differences was also low for the different monthly series. Moreover, the comparison of the sign and significance of the trends also show a similar pattern between observations and 'jack-knifing' predictions. Thus, the percentage of stations showing positive and significant trends in each month and annually is quite similar between observed and 'jack-knifing' predicted data (Figure S6) which suggests that air temperature trends obtained from the gridded data are not affected by the methodological procedure adopted.

Trends were also analysed for each 5×5 gridded cell over the whole Peru and maps summarizing the significance and trend were created. We calculated the surface area affected by positive and negative trends and by significant and non-significant changes. We also computed the temperature change and the significance of the trends at different elevation levels, using a 500 m interval.

3. Results

3.1. Maximum air temperature

Figure 7 illustrates the evolution of the average maximum air temperature in Peru for each monthly and annual series. It shows a positive trend for all months of the year, but more pronounced for the winter (JJA) months, given the highest trend for August, September and October. In January and February, the increase was statistically insignificant ($p > 0.05$). Annual maximum air temperature showed a statistically significant increase on the order of 0.18 °C decade^{-1}. Figure 8 shows the monthly and annual spatial distribution of the trend for maximum air temperature. The spatial patterns are very homogeneous in December and January, with few differences among the different regions. A cooling trend is observed over the Amazonian basin to the northeast from February to May, whereas warming conditions prevailed in the Andean region. The increase in maximum air temperatures is clearly reinforced during the extended cold season (JJASON), as air maximum temperatures noticeably increased in the Andean region. Significant positive trends in maximum air temperature were dominant in the majority of Peru (Figure S7), with the exception of areas of the Amazonian basin that showed less warming during summer months. Over these months the trends were either positive, though being statistically insignificant, or negative (Figure S8).

Figure 9 illustrates the trend in maximum air temperature, plotted as a function of different elevation intervals for the period 1964–2014. Low elevations (<500 m) represent a high percentage of the total surface of the country (50.5%), but they are represented by only 23.5% of the available observatories, suggesting that uncertainty of the obtained trend could be higher in low elevated areas. On the contrary, between 1000 and 4500 m, there is good representation of meteorological stations, leading to a lower uncertainty of the obtained trends from the gridded layers.

In any case, results reveal a clear topographic gradient at the annual scale, which is consistent with the dominant pattern observed between March and November. In contrast, there was no clear topographic gradient for the observed warming trends between December and February, although the areas located below 500 m.a.s.l. showed weaker trends. Notably, lower warming magnitude was recorded at low elevated areas (<500 m.a.s.l.) from March to November, which varies on average between 0.06 °C decade^{-1} in June and 0.2 °C decade^{-1} in September. Nevertheless, there is a progressive increase of the observed trends as elevation increases. For example, at the elevation range between 2500 and 3000 m.a.s.l., the maximum air temperature increase in September was 0.34 °C decade^{-1}, while it was higher than 0.4 °C decade^{-1} at 5000 m.a.s.l. This pattern suggests that the Peruvian territory above 500 m.a.s.l. showed positive and significant trends of maximum air temperature from March to November: a finding that is confirmed in Figure S9.

3.2. Minimum air temperature

The regional average of the minimum air temperature series for the whole Peru exhibited positive and significant trends for all months of the year (Figure 10). The main increase was recorded in December (0.22 °C decade^{-1}), while the lowest increase was observed in August and September (0.10 and 0.12 °C decade^{-1}, respectively). Annually, the increase was on the order of 0.16 °C decade^{-1}, which is closer to the trend found for the maximum air temperatures (0.18 °C decade^{-1}). The spatial pattern of the magnitude changes was more homogeneous than those found for the maximum air temperatures (Figure 11). At the annual scale, there were no differences between the Andes, the Amazonian region and the Pacific coastland. At the monthly scale, the main spatial differences were recorded in September, where the southern areas of the Andes showed a dominant cooling trend. Also, some cooling was identified in the Andean region in August. Generally, the positive and significant changes were dominant throughout the entire country during the majority of months (Figures S10 and S11). The spatial pattern of minimum air temperature trends shows strong differences when compared to maximum air temperature trends. The trend in minimum air temperatures did not show an increase as a function of elevation, but generally decreased in most months of the year and at the annual scale. Nevertheless, the differences among different elevation thresholds were lower than those found

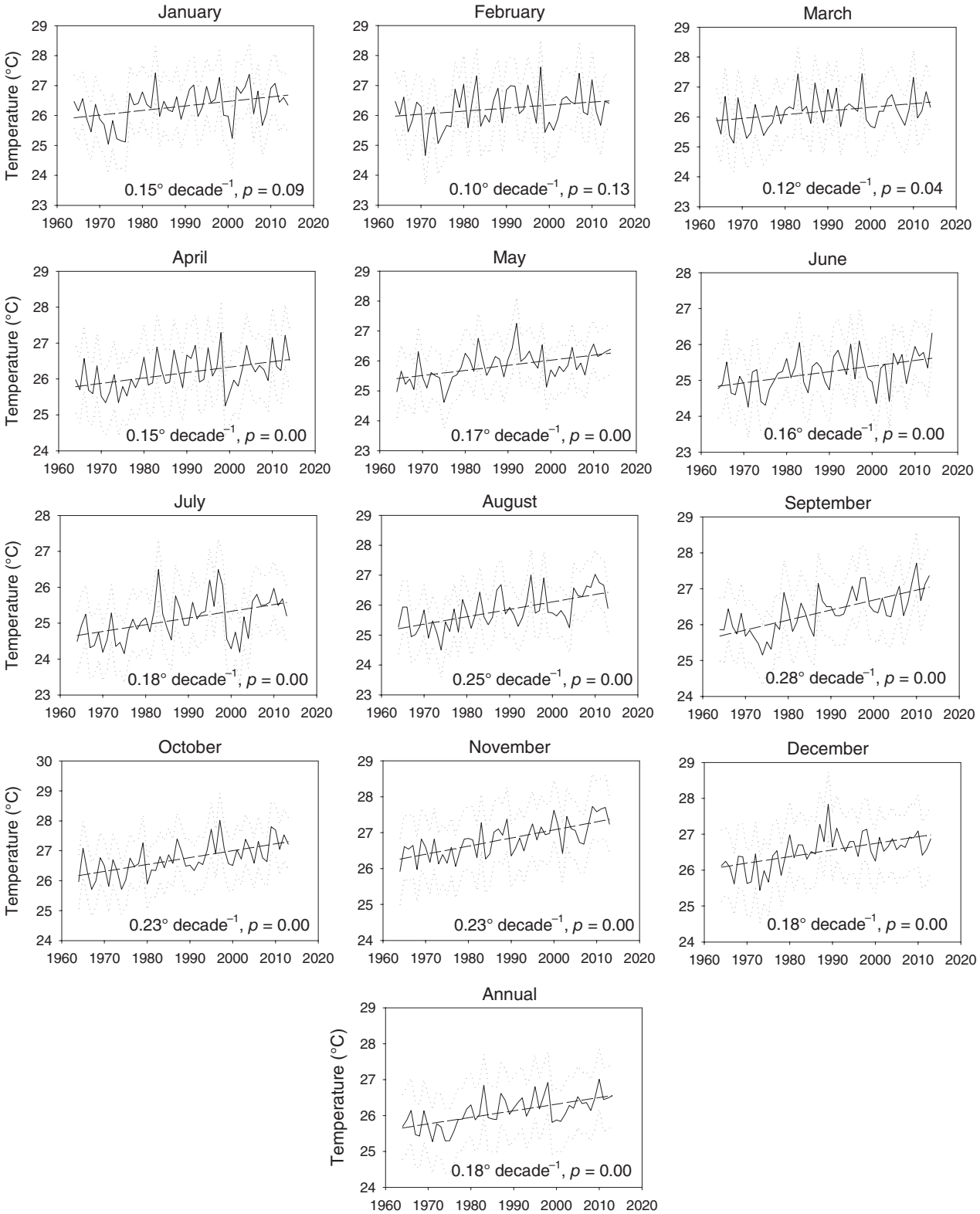

Figure 7. Monthly and annual evolution of the average maximum air temperature over Peru. The linear fitting is shown by dashed lines. The trend is given in °C decade^{-1}. Standard error of the average is provided in grey dotted lines.

for the maximum air temperature (Figure 12). For minimum air temperature, the trend was more important at low elevated areas. Thus, at elevations above 3000 m.a.s.l., the percentage of surface showing positive and significant trends was low between May and September (Figure S12).

3.3. Mean air temperature

In agreement with the observed trends for maximum and minimum air temperatures, the mean air temperature showed a dominant increase over Peru for the period 1964–2014. The monthly series showed a generally

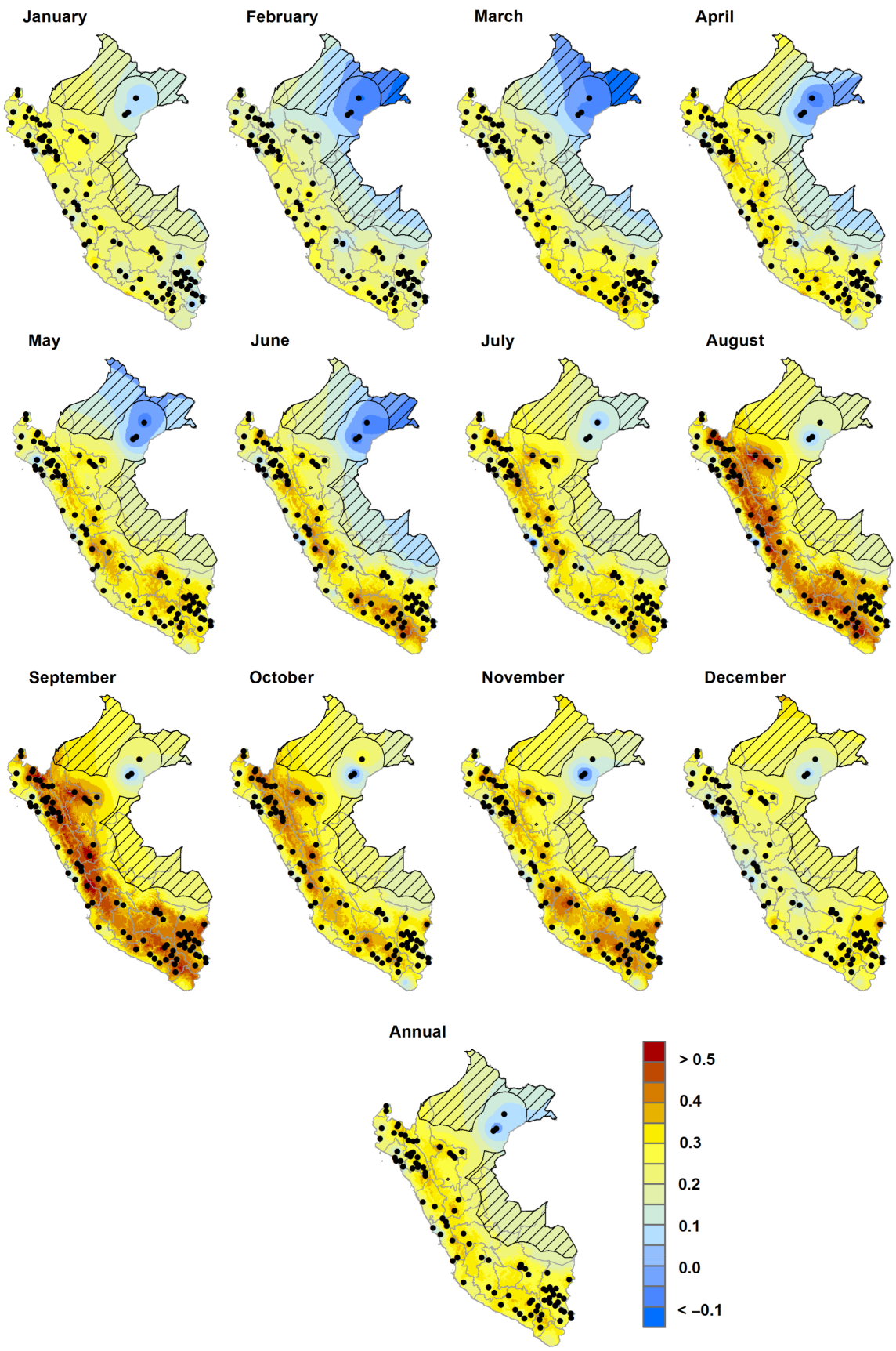

Figure 8. Spatial distribution of the monthly and annual trend (in °C decade^{-1}) of maximum air temperature. Shaded areas correspond to unsampled regions in which temperature trends show higher uncertainty. [Colour figure can be viewed at wileyonlinelibrary.com].

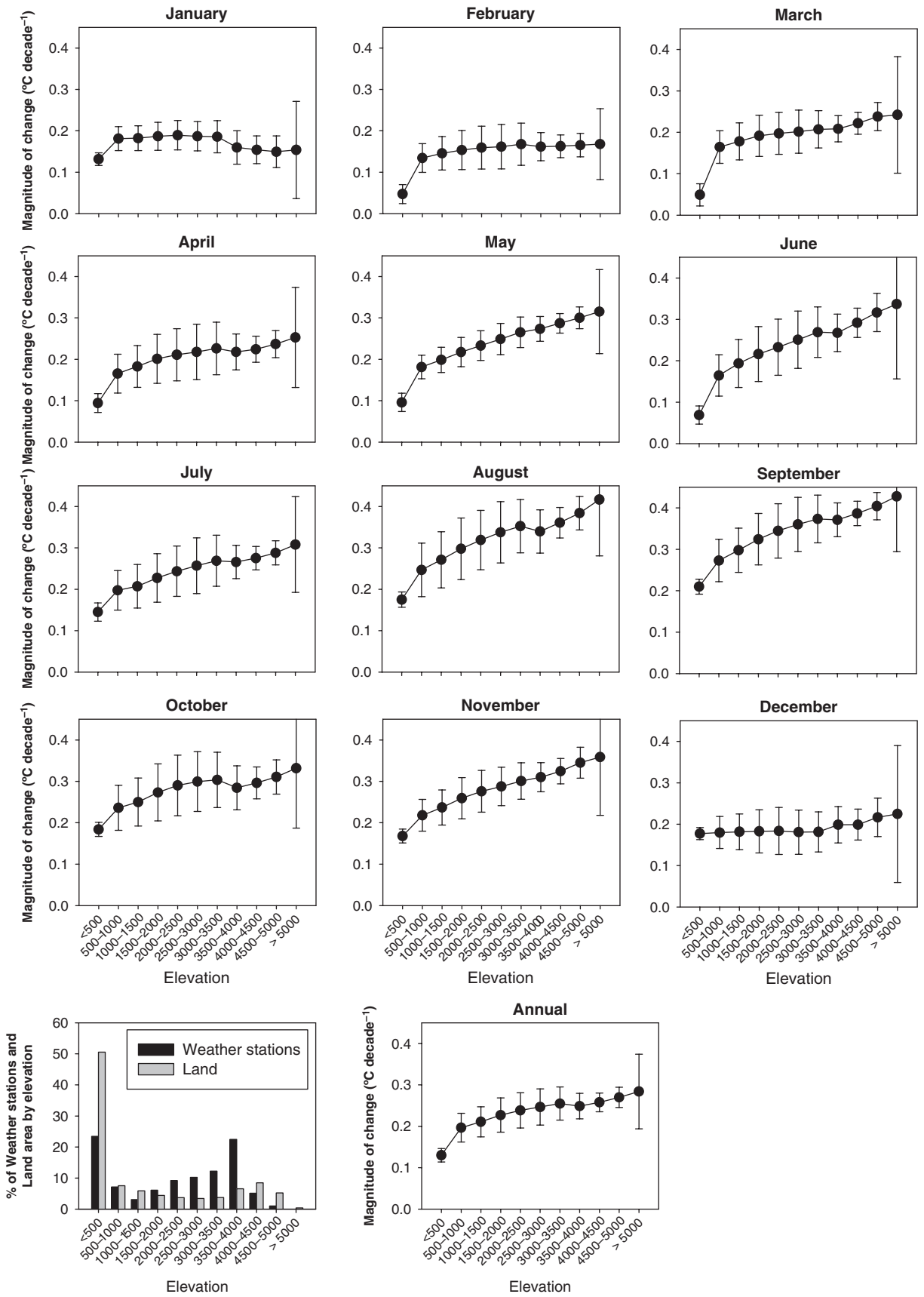

Figure 9. Monthly and annual average of the trend in maximum air temperature (in °C decade^{-1}) per different elevation intervals over Peru. Vertical bars represent the standard error of the average multiplied by 50 to be visible. The left bottom plot compares the percentage of land and percentage of meteorological stations in the different elevation intervals.

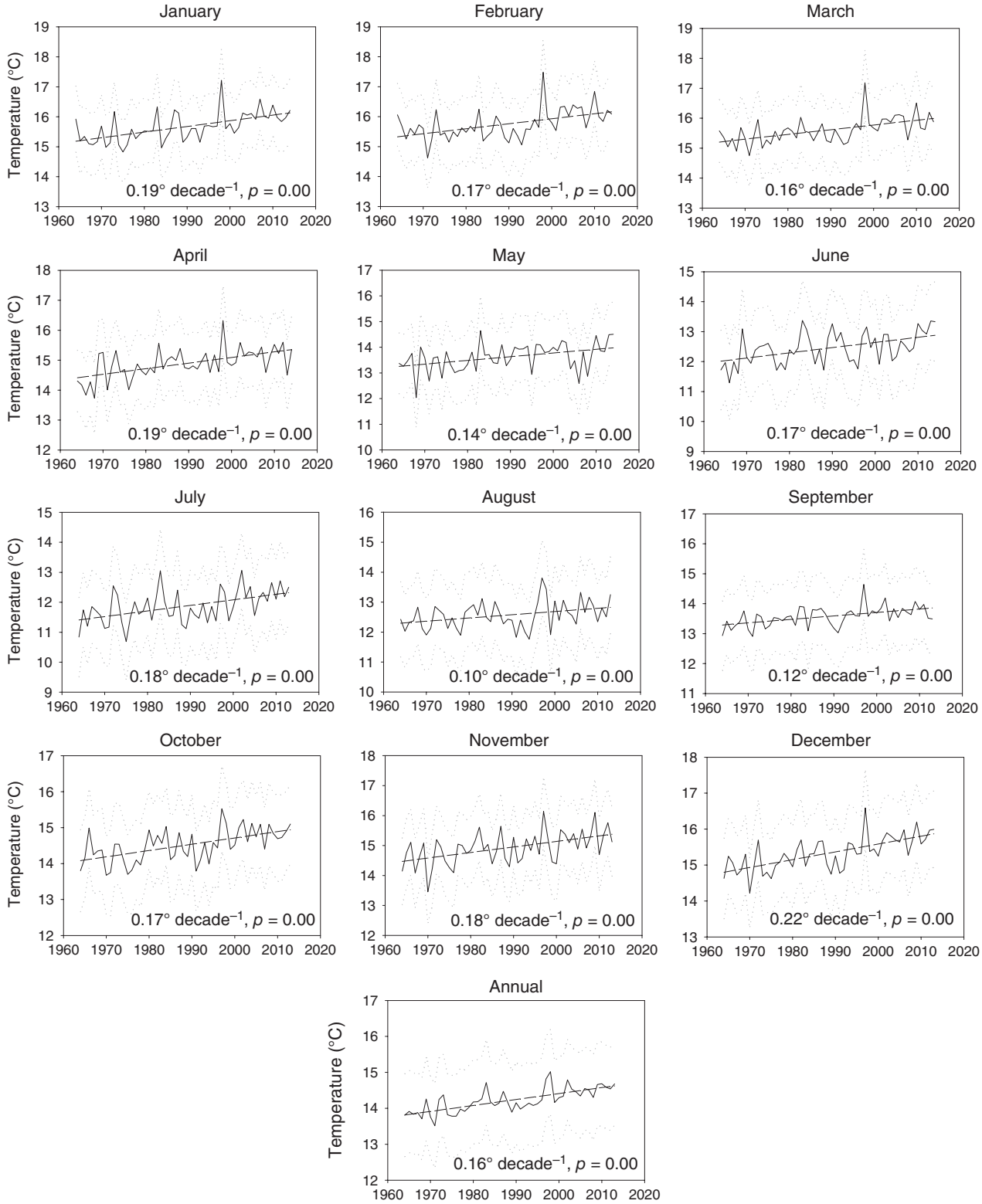

Figure 10. As in Figure 7, but for minimum air temperature.

positive and significant increase, being more pronounced between September and December (0.2 °C decade^{-1} on average). At the annual scale, the average increase over Peru was 0.17 °C decade^{-1} (Figure 13). Moreover, the spatial increase was very homogeneous over the different regions of Peru (Figure 14) and the positive and significant trends dominated over most of the country either monthly or annually (Figures S13 and S14).

The different response of the observed changes in maximum and minimum air temperatures to the elevation gradients would explain why there were no noticeable elevation gradients for the mean air temperature change

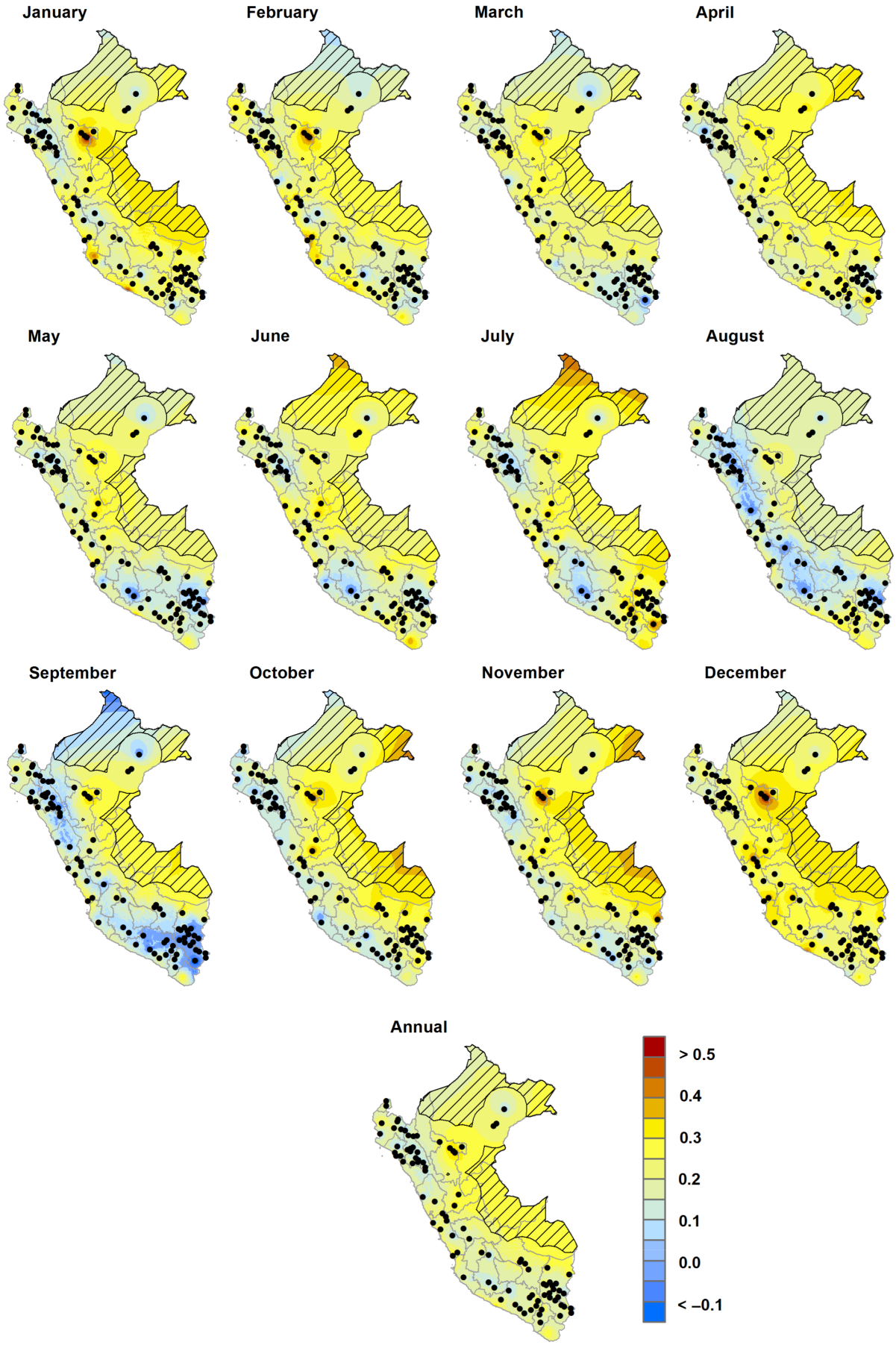

Figure 11. As in Figure 8, but for minimum air temperature. [Colour figure can be viewed at wileyonlinelibrary.com].

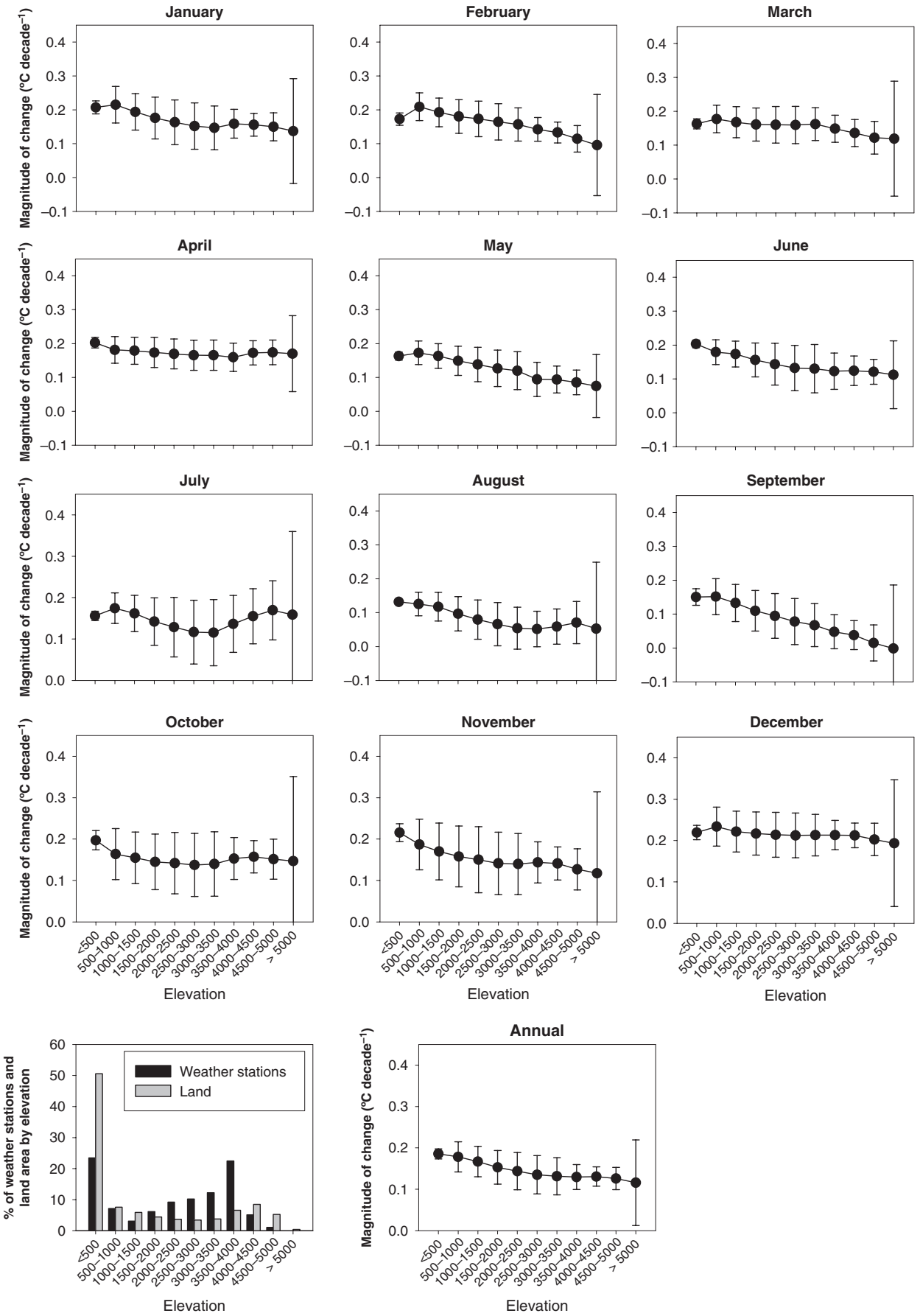

Figure 12. As in Figure 9, but for minimum air temperature.

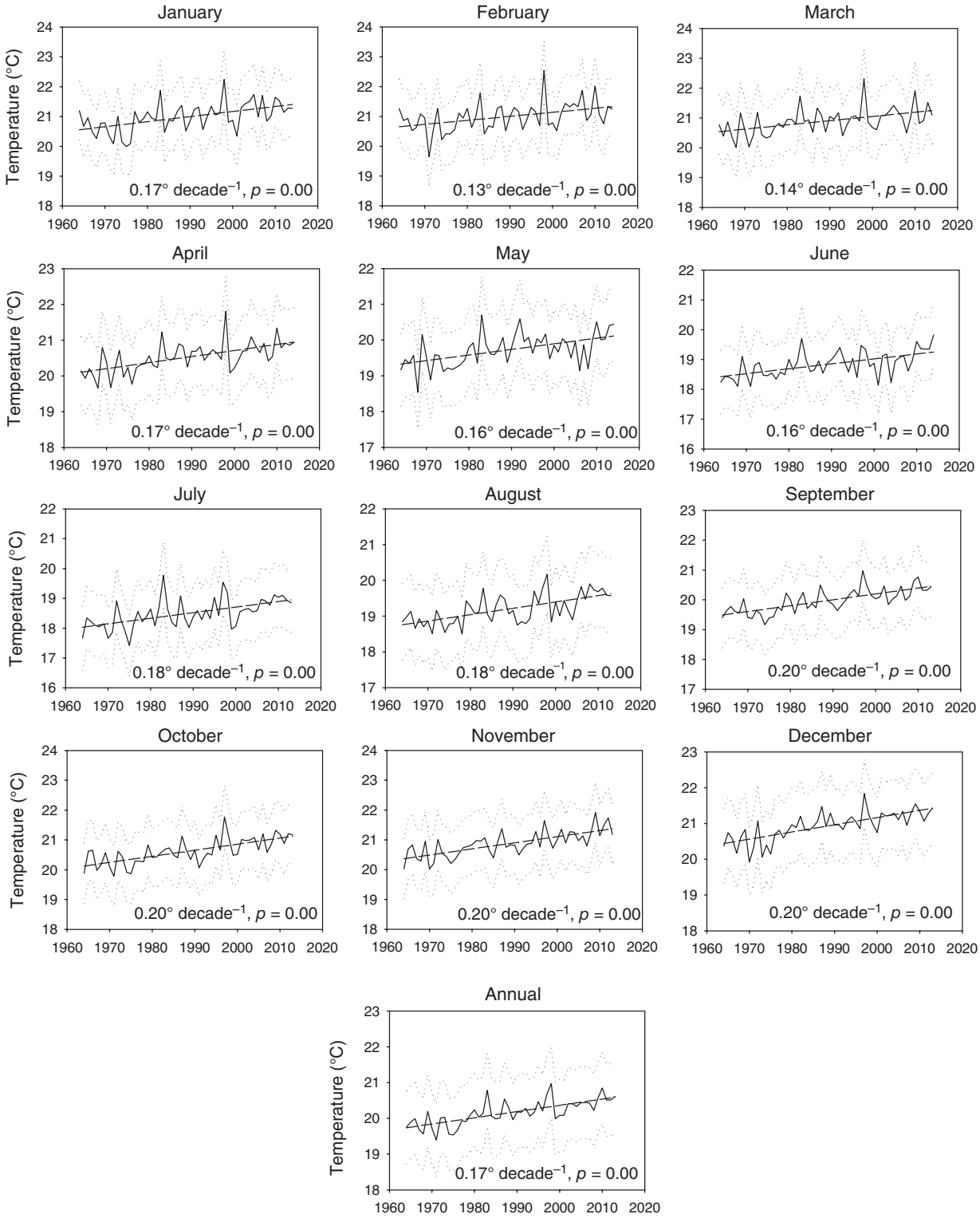

Figure 13. As in Figure 7, but for mean air temperature.

in Peru (Figure 15). In some months, there was a tendency toward a relatively lower trend at high elevations (e.g. January) or the opposite (e.g. June–August). Results also reveal that the differences in the trend were small at the monthly and annual scales, with no clear differences at the different elevation gradients. Indeed, the entire (100%) surface at different elevations showed positive and significant trends in mean air temperature across Peru (Figure S15).

4. Discussion and conclusions

In this study, we analysed recent air temperature changes in Peru for the period 1964–2014. To our knowledge,

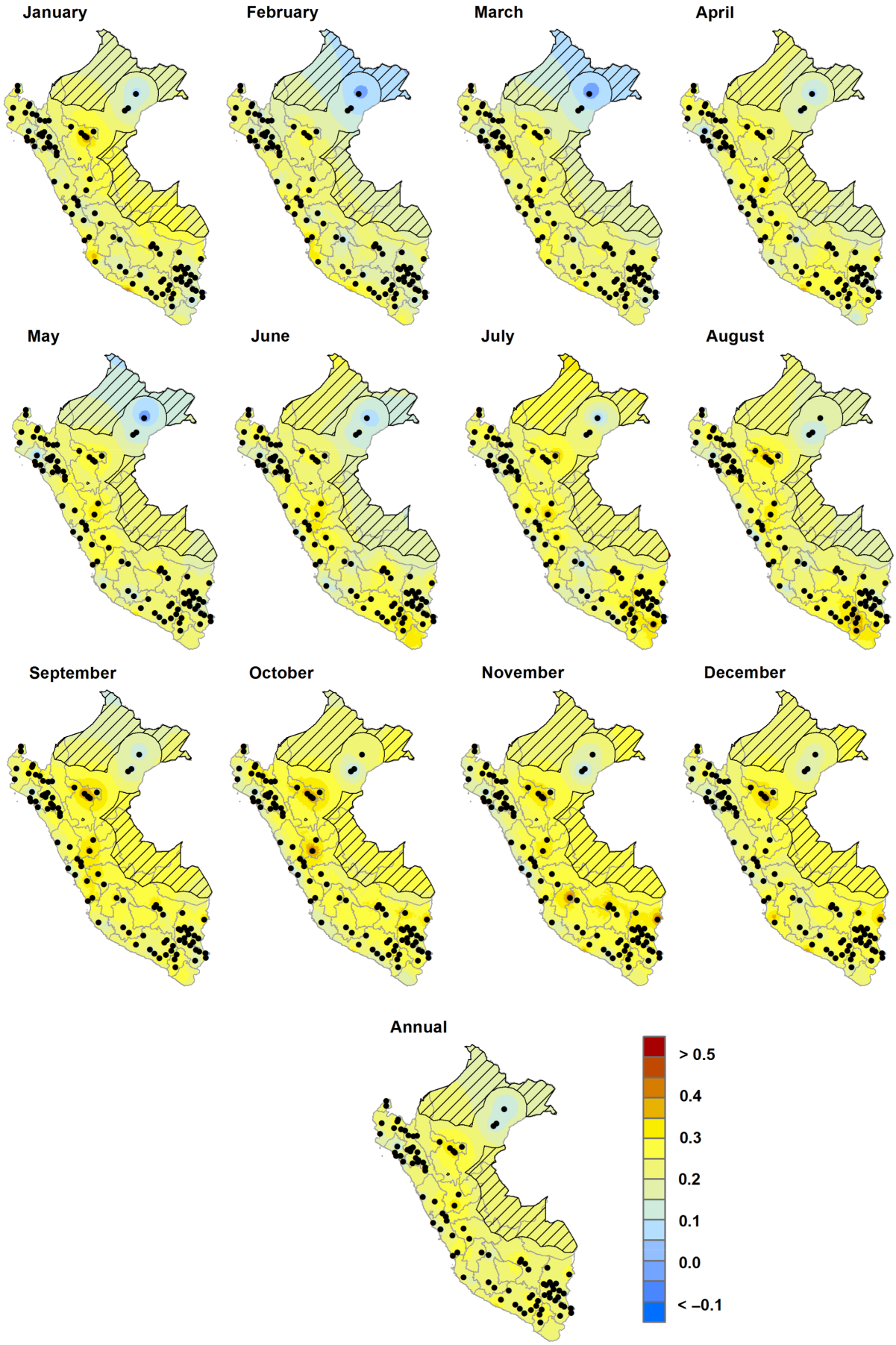

Figure 14. As in Figure 8, but for mean air temperature. [Colour figure can be viewed at wileyonlinelibrary.com].

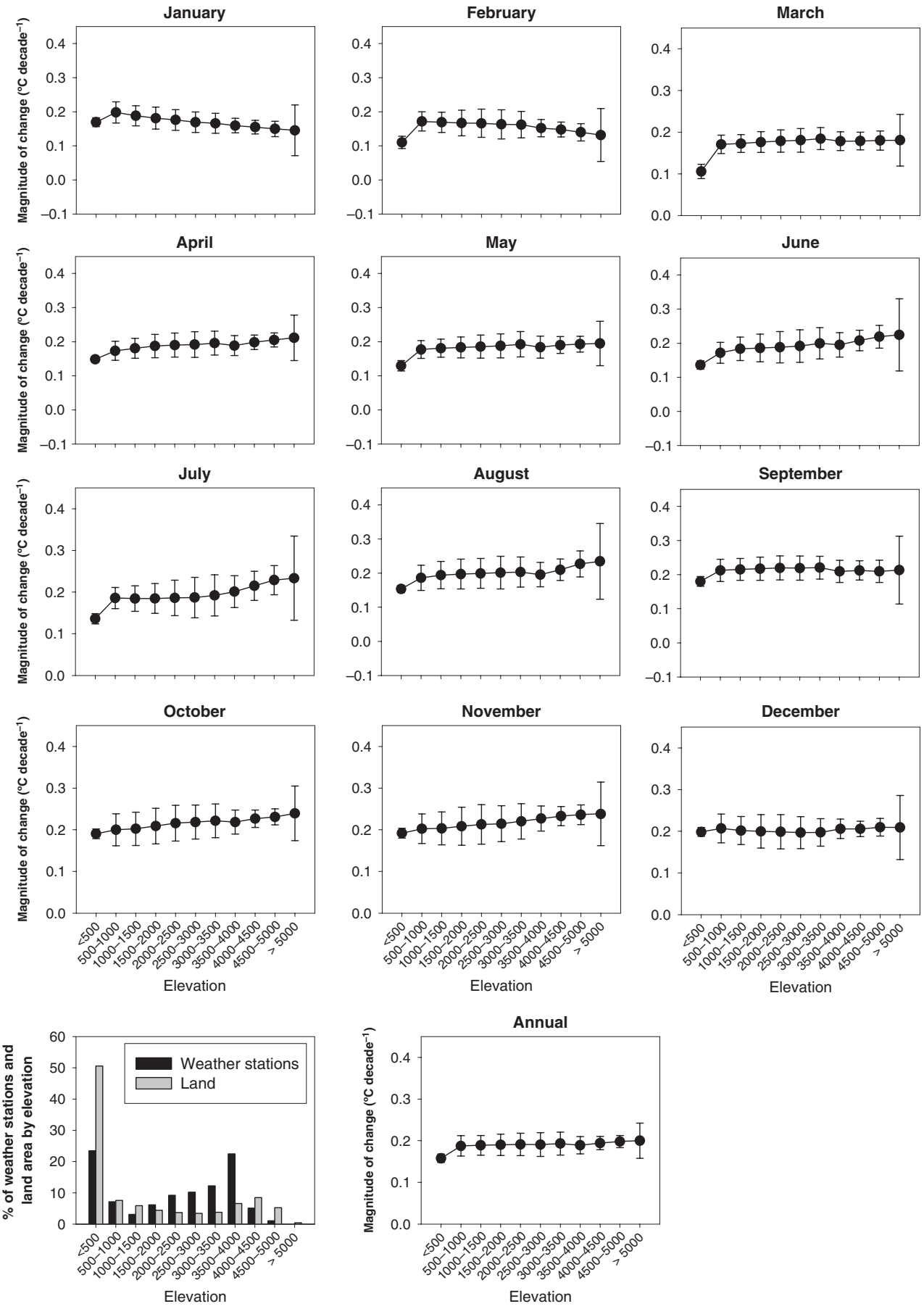

Figure 15. As in Figure 9, but for mean air temperature.

this is the first study that used the complete set of available air temperature records to analyse high spatial resolution trends across Peru. The first part of this study focussed on developing a complete, quality controlled and homogenized data set on which accurate gridded data were produced. We ensured that the majority of maximum and minimum air temperature series was homogeneous or had a low number of inhomogeneities. The defined break points were corrected prior to developing the gridded air temperature data sets and analysing temperature trends.

Here, we created the first quality controlled high-resolution gridded temperature data set for Peru at a 5×5 km spatial resolution. As the topography of Peru is very complex, our interpolation technique properly accounted for the possible impacts of relief on the spatial distribution of air temperature. The development of this spatially detailed data set over Peru overcomes the current limitations related to the lack of available high-resolution gridded air temperature series in the region. Limitations of available low-resolution global gridded data sets in the region has been addressed in previous studies. For example, Rusticucci *et al.* (2014) compared different low-resolution gridded data sets over the southern central Andes in South America (e.g. the Climate Research Unit data set and the ERA-Interim reanalysis), demonstrating potential shortcomings in these information sources. These results are in agreement with the results of Hofer *et al.* (2012), who compared the performance of different reanalysis data sets in the Cordillera Blanca, suggesting limitations in the horizontal grid resolution of these reanalyses and different seasonal skill of the data. Moreover, the available low-resolution grids showed little agreement on the variability of maximum air temperature, with an underestimation of the intensity of extremes, mainly near the Andes (Rusticucci *et al.*, 2010). The gridded data set created in this study shows high accuracy and low errors, in comparison with observational data. These errors are generally random in space and time, with no biases induced by the relief distribution. This data set can be useful not only for analysing the spatial and temporal variability of climate, but also for assessing the impact of differential warming trends on a variety of agricultural and hydrological systems. This data set can be accessed and downloaded in the Spanish National Research Council Repository (http://digital.csic.es/handle/10261/139347?locale=en).

On average, for the whole Peru, the air temperature increase was recorded in all months of the year and annually both for maximum, minimum and mean air temperatures over the period 1964–2014. Annually, the average trend for maximum, minimum and mean air temperatures was 0.18, 0.16 and 0.17 °C decade^{-1}, respectively. These warming magnitudes are similar to those found by other authors in some regions of Peru. For example, Vuille and Bradley (2000) analysed mean air temperature trends in the tropical Andes between 1939 and 1998, showing an increase of 0.11 °C decade^{-1}, albeit with a stronger warming rate since the 1970s (0.33 °C decade^{-1}). A similar warming rate was also reported by Mark and Seltzer (2005), Rabatel *et al.* (2013) and Vuille *et al.* (2008) for the last decades. Other studies have also shown a general warming trend in some particular areas of Peru. One example is López-Moreno *et al.* (2016) who suggested a warming trend in maximum air temperature at a rate of 0.15 °C decade^{-1} from 1965 to 2012 in the Altiplano and the surrounding Andean slopes of Bolivia and Peru. Schauwecker *et al.* (2014) showed a strong air temperature rise in the Cordillera Blanca (0.31 °C decade^{-1}) between 1969 and 1998, and a weaker warming (0.13 °C decade^{-1}) from 1983 to 2012. More recently, Vuille *et al.* (2015) analysed the possible impact of the recent global warming hiatus (Kosaka and Xie, 2013) on the air temperature evolution in the Andes, suggesting a general downward trend in the past two decades, which is also dependent on the elevation and distance to the Pacific Ocean.

Some studies have suggested that trends in the West Andean slopes close to the Pacific coastland show weaker warming in comparison to the eastern slopes (Vuille and Bradley, 2000; Falvey and Garreaud, 2009; De Jong *et al.*, 2016). In Peru, we have found that this pattern is mainly driven by the behaviour of minimum air temperatures during the majority of months and annually (Figure 16), having a significant effect on the differential warming in mean air temperature from September to January since maximum air temperatures in summer months show an opposite pattern characterized by stronger warming in the West Pacific slopes. In general, although the trend at the annual scale is similar to that reported by other authors in the Andean region, we found strong spatial and monthly differences in the trend and in the behaviour of both maximum and minimum air temperatures. On average, the maximum air temperatures increased mostly during the extended winter months, with stronger increase in August and September (0.25 and 0.28 °C decade^{-1}, respectively). In the warm season, the maximum air temperature increase varied between 0.10 and 0.18 °C, depending on the month of the year. This pattern is opposite to minimum air temperature, which showed the main increase during the warm season with the strongest increase in December (0.22 °C decade^{-1}). The homogeneous warming observed in the mean air temperature among the different months of the year can thus be explained by a compensation of the behaviour of intra-annual trends in maximum and minimum air temperatures. Few studies have focused on the analysis of maximum and minimum air temperatures in Peru, although a different evolution of maximum and minimum air temperatures at seasonal scale has been also stressed by Schauwecker *et al.* (2014) and López-Moreno *et al.* (2016). In the Cordillera Blanca, Schauwecker *et al.* (2014) suggested that the higher seasonal differences in the air temperature trends since 1964 are recorded for minimum than for maximum air temperatures. Nevertheless, recalling the important monthly differences found in each season, both in the trend as well as the spatial patterns, a comparison of the warming rates suggested in these studies is a difficult task.

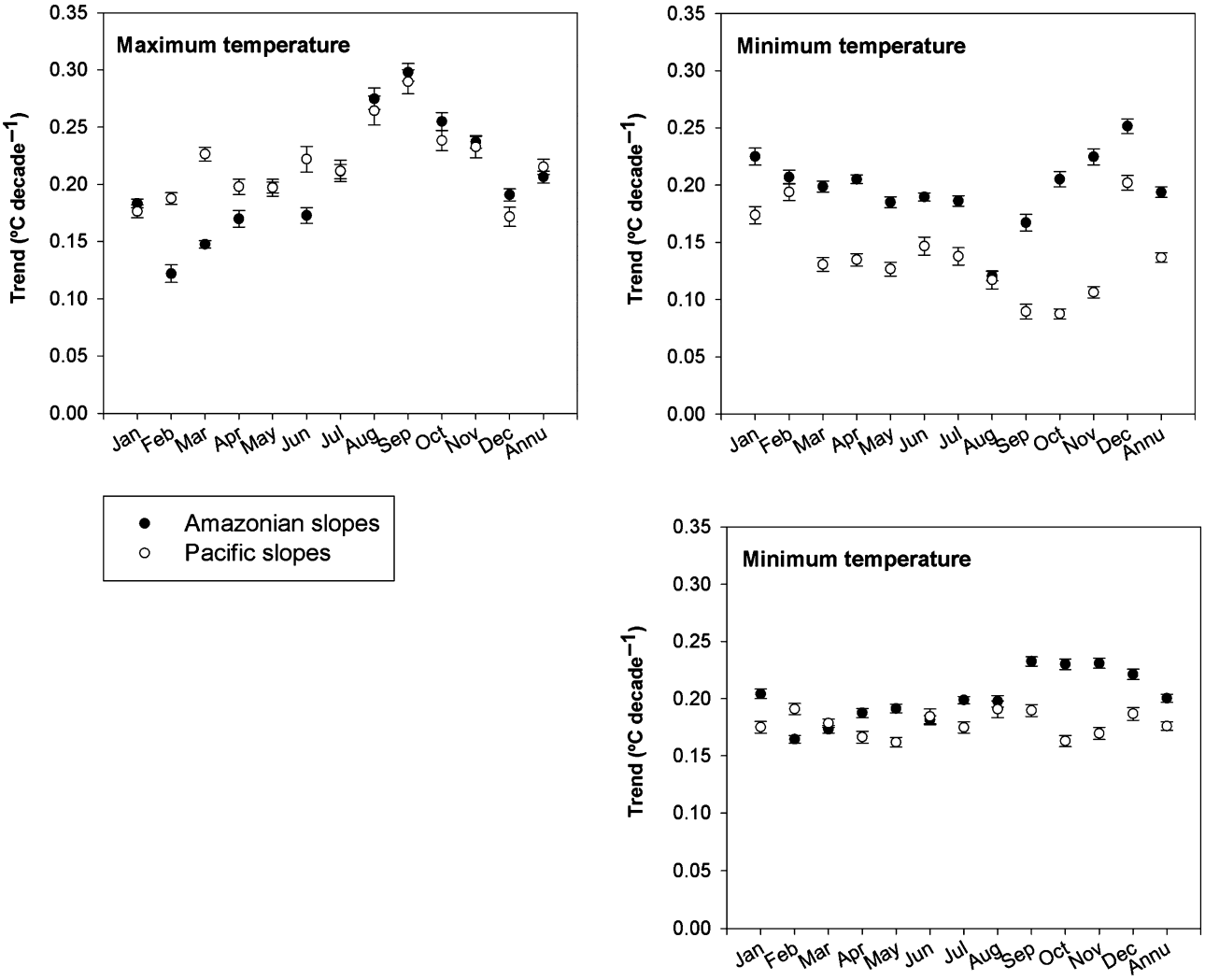

Figure 16. Average and standard error in monthly and annual maximum, minimum and mean air temperature trends in the Amazonian slopes and the Pacific slopes marked in Figure 1.

In addition to the seasonal differences in the evolution of maximum and minimum air temperatures, we found strong spatial differences in the trend, mostly determined by the elevation gradients in the region. A different warming trend driven by the elevation has been suggested by previous studies in different mountain regions worldwide (e.g. Beniston *et al.*, 1997; Diaz and Bradley, 1997; Pepin and Lundquist, 2008). In Peru, we demonstrated a clear different pattern in the behaviour of the maximum and minimum air temperature trends as a function of the elevation. Maximum air temperature shows a higher trend with elevation. Thus, the annual trend at the sea level is 0.13 °C decade^{-1}, compared to 0.21 °C decade^{-1} between 1000 and 1500 m.a.s.l., and 0.27 °C decade^{-1} at 4500 m.a.s.l. The strong increase of the maximum air temperatures in the mountain areas of Peru has been suggested as the main factor of the significant glacier retreat in the region (Racoviteanu *et al.*, 2008; Vuille *et al.*, 2008; Rabatel *et al.*, 2013; López-Moreno *et al.*, 2014; Veettil *et al.*, 2016). The depletion of snowpack and the enhanced snow-albedo feedback is driven by the altitudinal dependence of the air temperature trends, as reported in earlier works (Giorgi *et al.*, 1997). The increase of adiabatic processes in the mid- and high-troposphere is also related to temperature rise, particularly as a result of cloud condensation that affects latent/sensible ratios at high elevations (Ohmura, 2012). However, further research is needed to find a conclusive mechanism of this behaviour (Rangwala and Miller, 2012).

The strong altitudinal gradient in the warming conditions seems to be a general pattern of other Andean regions. For example, in the subtropical west coast of South America, Falvey and Garreaud (2009) showed a strong contrasted behaviour, with cooling at surface coastal stations (−0.2 °C decade^{-1}) and warming in the Andes (0.25 °C decade^{-1}), only 100–200 km further inland. Cooling air temperature trends in the Pacific South American coastland have been also identified in earlier works (e.g. Vuille and Bradley, 2000; De Jong *et al.*, 2016). Similar results have been recently obtained by Mernild *et al.* (2017) who have simulated snow conditions and trends for the entire Andes between 1979 and 2014,

indicating positive trends in air temperature in the high peaks, and negative trends at relatively lower elevations to the east and west of the Cordillera. This pattern concurs with the results obtained using the few meteorological stations available for the Peruvian eastern Amazonian region in this work. Nevertheless, the stronger warming pattern found for maximum air temperature at higher elevations is not identified for minimum air temperature. Minimum air temperature showed stronger warming rates in low elevated areas, compared to high elevations. As the amounts of change in minimum air temperature, as a function of elevation, are lower than those of maximum air temperature, low elevation differences in the warming trends of mean air temperature can be expected.

The slightly larger increase of maximum air temperatures than minimum air temperatures is mostly driven by the different spatial variability in their trends. While minimum air temperatures show a more homogeneous spatial pattern, maximum air temperatures exhibit a significant positive trend throughout most of the Andean region. This pattern has also been recently identified in Ecuador (Morán-Tejeda *et al.*, 2016) and it is related to the different altitudinal gradient in warming rates between minimum and maximum air temperatures. Falvey and Garreaud (2009) suggested that the variation in air temperature trends from the coast to the Andes is largely due to strong vertical stratification of air temperature trends in the lower troposphere west of the Andes, and pointed out that the coastal cooling could be related to El Niño-Southern Oscillation (ENSO) phenomenon and the trend of La Niña pattern. Vuille and Bradley (2000) stressed that high elevation stations in the Andes did not reflect the slight cooling trend that they identified in the tropical lower troposphere, with most of maximum air temperature series showing positive trends (López-Moreno *et al.*, 2014). Moreover, Vuille *et al.* (2015) suggested that this differential warming could be related to the Pacific Decadal Oscillation. The complex influence of the ENSO phenomenon in the region could explain the observed patterns, given the different influence of sea surface temperatures over the central (affecting the Andes Cordillera) and the eastern (affecting the coastland) Pacific (Morán-Tejeda *et al.*, 2016; Vicente-Serrano *et al.*, 2017). The physical mechanisms that control the different altitudinal ratio of warming between maximum and minimum air temperatures are unclear but probably ENSO trends can explain the higher warming in maximum air temperature trends in the Andes because of their major response to El Niño and La Niña phases in both the dry and humid seasons (López-Moreno *et al.*, 2014). This is caused by the ENSO that modulates other atmospheric parameters, such as surface air pressure, solar radiation and cloudiness in the Andes (Vuille, 1999; Vuille *et al.*, 2000). Nevertheless, further research is needed to better attribute the drivers explaining the different magnitude of warming at different elevations for maximum and minimum air temperatures across Peru, which is out of the scope of this manuscript.

The dominant warming trends observed for 1964–2014 are expected to intensify in the future. Different studies have used the global climate models (GCMs) forced by different greenhouse gas emission scenarios and downscaling techniques to determine the possible future warming trends in the Andean region. The majority of these studies projected a reinforcement of the warming conditions, with a strong air temperature increase by the end of the 21st century (e.g. Bradley *et al.*, 2004; Thibeault *et al.*, 2010; Sanabria and Lhomme, 2013). Following the SRES A2 emission scenario, Vuille *et al.* (2008) suggested that the tropical Andes may experience a massive warming on the order of 4.5–5 °C, with a likely stronger increase in air temperature at higher elevations. Bradley *et al.* (2004) analysed a suite of seven GCM simulations in South America with $2 \times CO_2$ levels and showed large air temperature changes compared to the run period. They showed that, independently of the latitude, the modelled warming trend increases with elevation. These results are in agreement with those of Urrutia and Vuille (2009), who used a regional climate model and two different emission scenarios in the tropical Andes to project an enhanced warming at higher elevations and further amplified in the middle and upper troposphere. Studies over particular mountain massifs of Peru also suggest a strong warming in highly elevated areas. Based on the most optimistic assumptions of greenhouse gas concentrations, López-Moreno *et al.* (2014) assessed climate simulations for the near future (2021–2050) over the Huaytapallana range, projecting a continuation of climate warming at a similar rate observed during the second half of the 20th century. Accordingly, any projected warming trends over Peru can cause a strong depletion of glaciers at the mid-21st century (Vuille *et al.*, 2008), changes in crop cycles (Sanabria and Lhomme, 2013) and a decrease of the permafrost extent by up to 95% (Rangecroft *et al.*, 2016). The consequences of the forecasted warming in Peru could be dramatic, given that the urban water consumption in the highly populated cities located in the Peruvian coastland and the agricultural areas in the lowlands depend mostly on water produced in the mountain ranges.

Acknowledgements

This work was supported by the research projects PCIN-2015-220, CGL2014-52135-C03-01, Red de variabilidad y cambioclimático RECLIM (CGL2014-517221-REDT) financed by the Spanish Ministry of Economy and Competitiveness and FEDER, 'IMDROFLOOD-Improved Drought and Flood Early Warning, Forecasting and Mitigation using real-time hydroclimatic indicators' supported by EU and Spanish Ministry of Economy and Competitiveness under the ERA-NET Cofund WaterWorks2014 Call. This ERA-NET is an integral part of the 2015 Joint Activities developed by the Water Challenges for a Changing World Joint Programme Initiative (Water JPI), Ephyslab (UVIGO-CSIC Associated Unit) and 'LIFE12 ENV/ES/000536-Demonstration and validation of innovative methodology for regional climate change adaptation

in the Mediterranean area (LIFE MEDACC)' financed by the LIFE programme of the European Commission.

Supporting information

The following supporting information is available as part of the online article:

Figure S1. Left: percentage of missing data in maximum and minimum air temperature. Right: percentage of data replaced by the homogeneity procedure in the selected stations.

Figure S2. Relationship between the monthly errors in the gridded layers and elevation (maximum air temperature).

Figure S3. Relationship between the monthly errors in the gridded layers and elevation (minimum air temperature).

Figure S4. Monthly spatial distribution of mean average error for maximum air temperatures in each meteorological station.

Figure S5. Monthly spatial distribution of mean average error for minimum air temperatures in each meteorological station.

Figure S6. Percentage of stations showing positive and significant ($p < 0.05$) and positive and non-significant ($p > 0.05$) trends for maximum, minimum and mean air temperature.

Figure S7. Percentage of surface area in Peru assigned to the different classes of the significance of maximum air temperature changes.

Figure S8. Spatial distribution of the trends in maximum air temperature. Shaded areas correspond to unsampled regions in which temperature trends show higher uncertainty.

Figure S9. Percentage of surface with positive and negative trends in monthly and annual maximum air temperature per different elevation intervals in Peru.

Figure S10. As in Figure S3, but for minimum air temperature.

Figure S11. As in Figure S4 but for minimum air temperature.

Figure S12. As in Figure S5, but for minimum air temperature.

Figure S13. As in Figure S3, but for minimum air temperature.

Figure S14. As in Figure S4, but for mean air temperature.

Figure S15. As in Figure S5, but for mean air temperature.

Table S1. Number of stations with significant differences in the magnitude of air temperature trends comparing observations and predictions by the jack-knifing approach.

References

Abtew W, Melesse A. 2013. *Climate Change and Evapotranspiration Evaporation and Evapotranspiration: Measurements and Estimations*. Springer Netherlands: Dordrecht, The Netherlands, 197–202.

Agnew MD, Palutikof JP. 2000. GIS-based construction of base line climatologies for the Mediterranean using terrain variables. *Clim. Res.* **14**: 115–127.

Azorin-Molina C, Vicente-Serrano SM, Sanchez-Lorenzo A, McVicar T, Morán-Tejeda E, Revuelto J, El Kenawy A, Martín-Hernández N, Tomas-Burguera M. 2015. Atmospheric evaporative demand observations, estimates and driving factors in Spain (1961-2011). *J. Hydrol.* **523**: 262–277.

Barros VRA, Boninsegna JAB, Camilloni IAA, Chidiak MC, Magrín GOD, Rusticucci ME. 2015. Climate change in Argentina: trends, projections, impacts and adaptation. *WIREs Clim. Change* **6**: 151–169.

Basist A, Bell GD, Meentemeyer V. 1994. Statistical relationships between topography and precipitation patterns. *J. Clim.* **7**: 1305–1315.

Beniston M, Diaz HF, Bradley RS. 1997. Climatic change at high elevation sites: an overview. *Clim. Change* **36**: 233–251.

Bennett M, New M, Marino J, Sillero-Zubiri C. 2016. Climate complexity in the Central Andes: a study case on empirically-based local variations in the Dry Puna. *J. Arid Environ.* **128**: 40–49.

Bradley RS, Keimig FT, Diaz HF. 2004. Projected temperature changes along the American cordillera and the planned GCOS network. *Geophys. Res. Lett.* **31**(16): L162101–L162104.

Brown DP, Comrie AC. 2002. Spatial modeling of winter temperature and precipitation in Arizona and New Mexico, USA. *Clim. Res.* **22**: 115–128.

Brunetti M, Maugeri M, Monti F, Nanni T. 2006. Temperature and precipitation variability in Italy in the last two centuries from homogenised instrumental time series. *Int. J. Climatol.* **26**: 345–381.

Burke EJ. 2011. Understanding the sensitivity of different drought metrics to the drivers of drought under increased atmospheric CO_2. *J. Hydrometeorol.* **12**: 1378–1394.

Carey M. 2005. Living and dying with glaciers: people's historical vulnerability to avalanches and outburst floods in Peru. *Global Planet. Change* **47**: 122–134.

Dai A. 2011. Drought under global warming: a review. *WIREs Clim. Change* **2**: 45–65.

Dai S, Shulski MD, Hubbard KG, Takle ES. 2016. A spatiotemporal analysis of Midwest US temperature and precipitation trends during the growing season from 1980 to 2013. *J. Clim. Appl. Meteorol.* **36**: 517–525.

Daly C, Neilson RP, Phillips DL. 1994. A statistical topographic model for mapping climatological precipitation over mountain terrain. *J. Appl. Meteorol.* **33**: 140–158.

Daly C, Gibson WP, Taylor GH, Johnson GL, Pasteris P. 2002. A knowledge-based approach to the statistical mapping of climate. *Clim. Res.* **22**: 99–113.

De Jong R, Schneider T, Hernández-Almeida I, Grosjean M. 2016. Recent temperature trends in the South Central Andes reconstructed from sedimentary chrysophytestomatocysts in Laguna Escondida (1742 m a.s.l., 38°28S, Chile). *Global Planet. Change* **137**: 24–34.

Diaz HF, Bradley RS. 1997. Temperature variations during the last century at high elevation sites. *Clim. Change* **36**: 253–279.

El Kenawy A, López-Moreno JI, Vicente-Serrano SM, Morsi F. 2010. Climatological modeling of monthly air temperature and precipitation in Egypt through GIS techniques. *Clim. Res.* **42**: 161–176.

El Kenawy A, López-Moreno JI, Vicente-Serrano SM. 2013. Summer temperature extremes in northeastern Spain: spatial regionalization and links to atmospheric circulation (1960–2006). *Theor. Appl. Climatol.* **113**: 387–405.

Falvey M, Garreaud RD. 2009. Regional cooling in a warming world: recent temperature trends in the southeast Pacific and along the west coast of subtropical South America (1979-2006). *J. Geophys. Res. Atmos.* **114**(4): D04102.

García NO. 1994. South American climatology. *Quat. Int.* **21**: 7–27.

Garreaud RD. 2009. The Andes climate and weather. *Adv. Geosci.* **22**: 3–11.

Garreaud RD, Vuille M, Compagnucci R, Marengo J. 2009. Present-day South American climate. *Palaeogeogr. Palaeoclimatol. Palaeoecol.* **281**: 180–195.

Giorgi F, Hurrell JW, Marinucci MR, Beniston M. 1997. Elevation dependency of the surface climate change signal: a model study. *J. Clim.* **10**: 288–296.

Gonzalez-Hidalgo JC, Peña-Angulo D, Brunetti M, Cortesi N. 2016. Recent trend in temperature evolution in Spanish mainland (1951–2010): from warming to hiatus. *Int. J. Climatol.* **36**(6): 2405–2416. https://doi.org/10.1002/joc.4519.

Goyal RK. 2004. Sensitivity of evapotranspiration to global warming: a case study of arid zone of Rajasthan (India). *Agric. Water Manag.* **69**: 1–11.

Hair JF, Anderson RE, Tatham RL, Black WC. 1998. *Multivariate Data Analysis*. Prentice Hall International Inc.: New York, NY, 799 pp.

Hamed KH, Rao AR. 1998. A modified Mann Kendall trend test for autocorrelated data. *J. Hydrol.* **204**: 182–196.

Hartmann DL, Klein Tank AMG, Rusticucci M, Alexander LV, Brönnimann S, Charabi Y, Dentener FJ, Dlugokencky EJ, Easterling DR, Kaplan A, Soden BJ, Thorne PW, Wild M, Zhai PM. 2013. Observations: atmosphere and surface. In *Climate Change 2013: The Physical Science Basis. Contribution of Working Group I to the Fifth Assessment Report of the Intergovernmental Panel on Climate Change*, Stocker TF, Qin D, Plattner G-K, Tignor M, Allen SK, Boschung J, Nauels A, Xia Y, Bex V, Midgley PM (eds). Cambridge University Press: Cambridge, UK and New York, NY.

Hofer M, Marzeion B, Mölg T. 2012. Comparing the skill of different reanalyses and their ensembles as predictors for daily air temperature on a glaciated mountain (Peru). *Clim. Dyn.* **39**: 1969–1980.

Holdaway MR. 1996. Spatial modeling and interpolation of monthly temperature using kriging. *Clim. Res.* **6**: 215–225.

Jones PD, Lister DH, Osborn TJ. 2012. Hemispheric and large-scale land-surface air temperature variations: an extensive revision and an update to 2010. *J. Geophys. Res. Atmos.* **117**(5): D05127.

Kosaka Y, Xie S-P. 2013. Recent global-warming hiatus tied to equatorial Pacific surface cooling. *Nature* **501**: 403–407.

Kunkel KE, Vose RS, Stevens LE. 2015. Is the monthly temperature climate of the United States becoming more extreme? *Geophys. Res. Lett.* **42**: 629–636.

Lanzante JR. 1996. Resistant, robust and non-parametric techniques for the analysis of climate data: theory and examples including applications to historical radiosonde station data. *Int. J. Climatol.* **16**: 1197–1226.

López-Moreno JI, Fontaneda S, Bazo J, Revuelto J, Azorin-Molina C, Valero-Garcés B, Morán-Tejeda E, Vicente-Serrano SM, Zubieta R, Alejo-Cochachín J. 2014. Recent glacier retreat and climate trends in Cordillera Huaytapallana, Peru. *Global Planet. Change* **112**: 1–11.

López-Moreno JI, Morán-Tejeda E, Vicente-Serrano SM, Bazo J, Azorin-Molina C, Revuelto J, Sánchez-Lorenzo A, Navarro-Serrano F, Aguilar E, Chura O. 2016. Recent temperature variability and change in the Altiplano of Bolivia and Peru. *Int. J. Climatol.* **36**: 1773–1796.

Mark BG, Seltzer GO. 2005. Evaluation of recent glacier recession in the Cordillera Blanca, Peru (AD 1962-1999): spatial distribution of mass loss and climatic forcing. *Quater Sci Rev* **24**: 2265–2280.

Martínez MD, Serra C, Burgueño A, Lana X. 2010. Time trends of daily maximum and minimum temperatures in Catalonia (NE Spain) for the period 1975–2004. *Int. J. Climatol.* **30**: 267–290.

McPhaden MJ, Vera CS, Martnez Guingla R. 2010. Climate variability and change in South America. *Eos* **91**: 473.

Mernild SH, Liston GE, Hiemstra CA, Malmros JK, Yde JC, Mcphee J. 2017. The Andes Cordillera. Part I: snow distribution, properties, and trends (1979-2014). *Int. J. Climatol.* **37**(4): 1680–1698.

Mestre O, Domonkos P, Picard F, Auer I, Robin S, Lebarbier E, Böhm R, Aguilar E, Guijarro J, Vertacnik G, Klancar M, Dubuisson B, Stepanek P. 2013. HOMER: HOMogenisation softwarE in R-methods and applications. *Idöjárás* **117**: 47–67.

Morán-Tejeda E, Bazo J, López-Moreno JI, Aguilar E, Azorín-Molina C, Sanchez-Lorenzo A, Martínez R, Nieto JJ, Mejía R, Martín-Hernández N, Vicente-Serrano SM. 2016. Climate trends and variability in Ecuador (1966-2011). *Int. J. Climatol.* **36**(11): 3839–3855.

Ninyerola M, Pons X, Roure JM. 2000. A methodological approach of climatological modelling of air temperature and precipitation through GIS techniques. *Int. J. Climatol.* **20**: 1823–1841.

Ohmura A. 2012. Enhanced temperature variability in high-altitude climate change. *Theor. Appl. Climatol.* **110**: 499–508.

Parmesan C, Yohe G. 2003. A globally coherent fingerprint of climate change impacts across natural systems. *Nature* **421**: 37–42.

Paternoster R, Brame R, Mazerolle P, Piquero AR. 1998. Using the correct statistical test for the equality of regression coefficients. *Criminology* **36**: 859–866.

Pepin NC, Lundquist JD. 2008. Temperature trends at high elevations: patterns across the globe. *Geophys. Res. Lett.* **35**(14): L14701.

Phillips DL, Dolph J, Marks D. 1992. A comparison of geostatistical procedures for spatial analysis of precipitation in mountainous terrain. *Agric. Meteorol.* **58**: 119–141.

Rabatel A, Francou B, Soruco A, Gomez J, Cáceres B, Ceballos JL, Basantes R, Vuille M, Sicart J-E, Huggel C, Scheel M, Lejeune Y, Arnaud Y, Collet M, Condom T, Consoli G, Favier V, Jomelli V, Galarraga R, Ginot P, Maisincho L, Mendoza J, Ménégoz M, Ramirez E, Ribstein P, Suarez W, Villacis M, Wagnon P. 2013. Current state of glaciers in the tropical Andes: a multi-century perspective on glacier evolution and climate change. *Cryosphere* **7**: 81–102.

Racoviteanu AE, Arnaud Y, Williams MW, Ordoñez J. 2008. Decadal changes in glacier parameters in the Cordillera Blanca, Peru, derived from remote sensing. *J. Glaciol.* **54**: 499–510.

Rangecroft S, Suggitt AJ, Anderson K, Harrison S. 2016. Future climate warming and changes to mountain permafrost in the Bolivian Andes. *Clim. Change* **137**: 231–243.

Rangwala I, Miller JR. 2012. Climate change in mountains: a review of elevation-dependent warming and its possible causes. *Clim. Change* **114**: 527–547.

Rusticucci M, Marengo J, Penalba O, Renom M. 2010. An intercomparison of model-simulated in extreme rainfall and temperature events during the last half of the twentieth century. Part 1: mean values and variability. *Clim. Change* **98**: 493–508.

Rusticucci M, Zazulie N, Raga GB. 2014. Regional winter climate of the southern central Andes: assessing the performance of ERA-Interim for climate studies. *J. Geophys. Res. Atmos.* **119**: 8568–8582.

Salzmann N, Huggel C, Rohrer M, Silverio W, Mark BG, Burns P, Portocarrero C. 2013. Glacier changes and climate trends derived from multiple sources in the data scarce Cordillera Vilcanota region, southern Peruvian Andes. *Cryosphere* **7**: 103–118.

Sanabria J, Lhomme JP. 2013. Climate change and potato cropping in the Peruvian Altiplano. *Theor. Appl. Climatol.* **112**: 683–695.

Schauwecker S, Rohrer M, Acuña D, Cochachin A, Dávila L, Frey H, Giráldez C, Gómez J, Huggel C, Jacques-Coper M, Loarte E, Salzmann N, Vuille M. 2014. Climate trends and glacier retreat in the Cordillera Blanca, Peru, revisited. *Global Planet. Change* **119**: 85–97.

Seiler C, Hutjes RWA, Kabat P. 2013. Climate variability and trends in Bolivia. *J. Appl. Meteorol. Climatol.* **52**: 130–146.

Simmons AJ, Willett KM, Jones PD, Thorne PW, Dee DP. 2010. Low-frequency variations in surface atmospheric humidity, temperature, and precipitation: inferences from reanalyses and monthly gridded observational data sets. *J. Geophys. Res. Atmos.* **115**(1): D01110.

Thibeault JM, Seth A, Garcia M. 2010. Changing climate in the Bolivian Altiplano: CMIP3 projections for temperature and precipitation extremes. *J. Geophys. Res. Atmos.* **115**(8): D08103.

Urrutia R, Vuille M. 2009. Climate change projections for the tropical Andes using a regional climate model: temperature and precipitation simulations for the end of the 21st century. *J. Geophys. Res. Atmos.* **114**(2): D02108.

Valdivia C, Thibeault J, Gilles JL, García M, Seth A. 2013. Climate trends and projections for the Andean Altiplano and strategies for adaptation. *Adv. Geosci.* **33**: 66–77.

Vecchi GA, Soden BJ. 2007. Global warming and the weakening of the tropical circulation. *J. Clim.* **20**: 4316–4340.

Vecchi GA, Soden BJ, Wittenberg AT, Held IM, Leetmaa A, Harrison MJ. 2006. Weakening of tropical Pacific atmospheric circulation due to anthropogenic forcing. *Nature* **441**: 73–76.

Veettil BK, Wang S, Bremer UF, de Souza SF, Simões JC. 2016. Recent trends in annual snowline variations in the northern wet outer tropics: case studies from southern Cordillera Blanca, Peru. *Theor. Appl. Climatol.* https://doi.org/10.1007/s00704-016-1775-0.

Venema VKC, Mestre O, Aguilar E, Auer I, Guijarro JA, Domonkos P, Vertacnik G, Szentimrey T, Stepanek P, Zahradnicek P, Viarre J, Müller-Westermeier G, Lakatos M, Williams CN, Menne MJ, Lindau R, Rasol D, Rustemeier E, Kolokythas K, Marinova T, Andresen L, Acquaotta F, Fratianni S, Cheval S, Klancar M, Brunetti M, Gruber C, Prohom Duran M, Likso T, Esteban P, Brandsma T. 2012. Benchmarking homogenization algorithms for monthly data. *Clim. Past* **8**: 89–115.

Vicente Serrano SM, Saz MA, Cuadrat JM. 2003. Comparative analysis of interpolation methods in the middle Ebro valley (Spain): application to annual precipitation and temperature. *Clim. Res.* **24**: 161–180.

Vicente-Serrano SM, Lanjeri S, López-Moreno JI. 2007. Comparison of different procedures to map reference evapotranspiration using geographical information systems and regression-based techniques. *Int. J. Climatol.* **27**: 1103–1118.

Vicente-Serrano SM, Beguería S, López-Moreno JI, García-Vera MA, Stepanek P. 2010. A complete daily precipitation database for North-East Spain: reconstruction, quality control and homogeneity. *Int. J. Climatol.* **30**: 1146–1163.

Vicente-Serrano SM, Azorin-Molina C, Sanchez-Lorenzo A, Revuelto J, López-Moreno JI, González-Hidalgo JC, Espejo F. 2014. Reference evapotranspiration variability and trends in Spain, 1961–2011. *Global Planet. Change* **121**: 26–40.

Vicente-Serrano SM, Aguilar E, Martínez R, Martín-Hernández N, Azorin-Molina C, Sanchez-Lorenzo A, El Kenawy A, Tomás-Burguera M, Moran-Tejeda E, López-Moreno JI, Revuelto J, Beguería S, Nieto JJ, Drumond A, Gimeno L, Nieto R. 2017. The

complex influence of ENSO on droughts in Ecuador. *Clim. Dyn.* **48**: 405–427.

Villalba R, Lara A, Boninsegna JA, Masiokas M, Delgado S, Aravena JC, Roig FA, Schmelter A, Wolodarsky A, Ripalta A. 2003. Large-scale temperature changes across the southern Andes: 20th-century variations in the context of the past 400 years. *Clim. Change* **59**: 177–232.

Vörösmarty CJ, Green P, Salisbury J, Lammers RB. 2000. Global water resources: vulnerability from climate change and population growth. *Science* **289**: 284–288.

Vuille M. 1999. Atmospheric circulation over the Bolivian Altiplano during dry and wet periods and extreme phases of the southern oscillation. *Int. J. Climatol.* **19**: 1579–1600.

Vuille M, Bradley RS. 2000. Mean annual temperature trends and their vertical structure in the tropical Andes. *Geophys. Res. Lett.* **27**: 3885–3888.

Vuille M, Bradley RS, Keimig F. 2000. Interannual climate variability in the Central Andes and its relation to tropical Pacific and Atlantic forcing. *J. Geophys. Res. Atmos.* **105**: 12447–12460.

Vuille M, Francou B, Wagnon P, Juen I, Kaser G, Mark BG, Bradley RS. 2008. Climate change and tropical Andean glaciers: past, present and future. *Earth Sci. Rev.* **89**: 79–96.

Vuille M, Franquist E, Garreaud R, LavadoCasimiro WS, Cáceres B. 2015. Impact of the global warming hiatus on Andean temperature. *J. Geophys. Res. Atmos.* **120**: 3745–3757.

Walther G-R, Post E, Convey P, Menzel A, Parmesan C, Beebee T, Fromentin J-M, Hoegh-Guldberg O, Bairlein F. 2002. Ecological responses to recent climate change. *Nature* **416**: 389–395.

Wang K, Dickinson RE, Liang S. 2012. Global atmospheric evaporative demand over land from 1973 to 2008. *J. Clim.* **25**: 8353–8361.

Wang Q, Fan X, Wang M. 2014. Recent warming amplification over high elevation regions across the globe. *Clim. Dyn.* **43**: 87–101.

Willett KM, Dunn RJH, Thorne PW, Bell S, de Podesta M, Parker DE, Jones PD, Williams CN. 2014. HadISDH land surface multi-variable humidity and temperature record for climate monitoring. *Clim. Past* **10**: 1983–2006.

Willmott CJ. 1982. Some comments on the evaluation of model performance. *Bull. Am. Meteorol. Soc.* **63**: 1309–1313.

Yin JH. 2005. A consistent poleward shift of the storm tracks in simulations of 21st century climate. *Geophys. Res. Lett.* **32**(18): 1–4, L18701.

